Molecular Biology of the Cell
Vol. 15, 4073–4088, September 2004

Endocytosis as a Mechanism for Tyrosine Kinase-dependent Suppression of a Voltage-gated Potassium Channel

Edmund Nesti, Brian Everill, and Anthony D. Morielli*

The University of Vermont College of Medicine, Burlington, VT 05405

Submitted November 5, 2003; Revised June 7, 2004; Accepted June 11, 2004
Monitoring Editor: Tony Hunter

The voltage-gated potassium channel Kv1.2 undergoes tyrosine phosphorylation-dependent suppression of its ionic current. However, little is known about the physical mechanism behind that process. We have found that the Kv1.2 alpha-subunit protein undergoes endocytosis in response to the same stimuli that evoke suppression of Kv1.2 ionic current. The process is tyrosine phosphorylation-dependent because the same tyrosine to phenylalanine mutation in the N-terminus of Kv1.2 that confers resistance to channel suppression (Y132F) also confers resistance to channel endocytosis. Overexpression of a dominant negative form of dynamin blocked stimulus-induced Kv1.2 endocytosis and also blocked suppression of Kv1.2 ionic current. These data indicate that endocytosis of Kv1.2 from the cell surface is a key mechanism for channel suppression by tyrosine kinases.

INTRODUCTION

Ion channels regulate a wide range of cellular processes, including development (Moody, 1998) and neuronal plasticity (Levitan, 1994; Alkon *et al.*, 1998; Stevens and Sullivan, 1998; Burke *et al.*, 1999). Accordingly, the activity of nearly all ion channels is under some form of posttranslational control, most commonly direct phosphorylation of the ion channel protein (Levitan, 1994; Ismailov and Benos, 1995; Burke *et al.*, 1999). The earliest and most extensively studied examples of posttranslational modification of ion channels involve serine/threonine phosphorylation. But it is now recognized that tyrosine phosphorylation modulates ion channel function as well (Levitan, 1994; Siegelbaum, 1994; Lev *et al.*, 1995; Burke *et al.*, 1999; Cayabyab *et al.*, 2000; Fadool *et al.*, 2000; Nitabach *et al.*, 2001). The *Shaker* family potassium channel Kv1.2 was the first voltage-gated channel found to be so regulated (Huang *et al.*, 1993). Since then, the number of ligand and voltage-gated ion channels identified as substrates for tyrosine kinase-dependent regulation has expanded to include calcium-, sodium-, chloride-, NMDA-, AMPA nicotinic acetylcholine-, and cyclic nucleotide-gated channels (Davis *et al.*, 2001). Importantly, other Kv1 family channels have been examined extensively in this regard, including Kv1.3 (Holmes *et al.*, 1996; Fadool and Levitan, 1998) and Kv1.5 (Holmes *et al.*, 1996).

Tyrosine phosphorylation of Kv1.2 can be triggered by M1 muscarinic acetylcholine receptor (mAChR) or EGF receptor activation (Huang *et al.*, 1993; Tsai *et al.*, 1997). But other stimuli, including protein kinase C (PKC) activation using phorbol 12-myristate 13-acetate (PMA) or elevated intracellular Ca can also trigger channel phosphorylation and suppression (Huang *et al.*, 1993). In addition to tyrosine kinase activation, M1 mAChRs stimulate the physical association of Kv1.2 with a receptor tyrosine phosphatase that can dephosphorylate the channel and restore its activity. Consistent with this, inhibiting tyrosines with pervanadate results in increased channel tyrosine phosphorylation and resultant channel suppression (Tsai *et al.*, 1999). Therefore, Kv1.2 activity is controlled by a dynamic balance between tyrosine kinase and phosphatase activities. Muscarinic receptor-induced suppression of Kv1.2 requires the activation of the small GTP-ase RhoA (Cachero *et al.*, 1998), which suggests a role for the cytoskeleton in channel suppression. Such a role was delineated by the subsequent discovery that the actin-binding protein cortactin binds to Kv1.2 and may have a key role in its regulation by tyrosine kinases (Hattan *et al.*, 2002). However, the physical mechanism by which tyrosine phosphorylation evokes channel suppression has remained unknown.

Endocytosis was originally thought to provide a means by which nutrients or other molecules in the extracellular space could be taken up into the cell. It is now understood that endocytosis is also an important mechanism for the regulation of a variety of membrane proteins. These include receptor tyrosine kinases (Schlessinger *et al.*, 1978), G-protein–coupled receptors (Higuchi *et al.*, 1982; Pals-Rylaarsdam *et al.*, 1997; Edwardson and Szekeres, 1999; Delaney *et al.*, 2002), and ion channels. Among the earliest reports of ion channel regulation by endocytosis was an article published in 1988 describing the effects of pinocytosis on a potassium current in macrophages (Ince *et al.*, 1988). Since then the number of ion channels shown to undergo endocytosis has grown considerably. Perhaps the most well studied are epithelial sodium channels, which help regulate ion reabsorption in the kidney (Rotin *et al.*, 2001). Ubuquitin-dependent endocytosis has emerged as a key means of regulating the surface expression of ENaC at the cell surface (Staub *et al.*, 1997, 2000). Disruption of that process by a mutation within the gene encoding ENaC is associated with Liddle's syndrome, a heritable form of human hypertension (Schild *et al.*, 1996). Ion reabsorption is also regulated by another ion

Article published online ahead of print. Mol. Biol. Cell 10.1091/mbc.E03–11–0788. Article and publication date are available at www.molbiolcell.org/cgi/doi/10.1091/mbc.E03–11–0788.

* Corresponding author. E-mail address: anthony.morielli@uvm.edu.

channel, Kir1.1. Mutations within this channel are associated Bartter's syndrome (Derst *et al.*, 1997; Vollmer *et al.*, 1998), a disease that also involves disrupted salt uptake in the kidney. Interestingly, and with significant relevance to the findings reported here, recent evidence indicates that suppression of Kir1.1 is regulated by tyrosine phosphorylation-dependent dynamin and clathrin-mediated endocytosis (Sterling *et al.*, 2002; Zeng *et al.*, 2002). In excitable cells, endocytosis can have a direct effect on membrane potential through effects on ligand-gated ion channels (St John and Gordon, 2001; Sheng and Kim, 2002). In the synapse, for example, this has been hypothesized to have an important role in plasticity associated with learning and memory (Carroll *et al.*, 1999, 2001). Voltage-gated ion channels also regulate membrane excitability; however, little is known about their regulation by endocytosis. Like Kir1.1, the voltage-gated Kv1.3 potassium channel undergoes tyrosine kinase-dependent suppression (Holmes *et al.*, 1996). In one study that considered endocytosis as a potential mechanism, no evidence was found that Kv1.3 internalization accompanied channel suppression (Fadool *et al.*, 1997). However, detection of endocytosis in those studies was limited to immunofluorescence experiments with sample sizes that may have been insufficient to resolve small but significant changes in surface channel levels (see *Discussion*). Thus, the possibility that Kv1.3 and related Kv1 family potassium channel suppression may involve endocytosis remains open.

Here we report that tyrosine phosphorylation of the voltage-gated ion channel Kv1.2 causes endocytosis of the channel protein and that this process constitutes a mechanism for Kv1.2 suppression. Stimuli that we have previously shown to evoke channel suppression also evoke channel endocytosis. A mutation within the N-terminus of Kv1.2 that confers resistance to phosphorylation-dependent suppression of Kv1.2 ionic current (Y132F) also confers resistance to channel endocytosis. Overexpression of a dominant negative form of dynamin, a protein required for many forms of endocytosis, blocks both channel endocytosis and channel suppression. Therefore, endocytosis of Kv1.2 appears to be a physical mechanism for tyrosine phosphorylation-dependent channel suppression.

MATERIALS AND METHODS

Materials

Antibody directed against the first extracellular loop of Kv1.2 (α-Kv1.2e) was purchased from Biosource International (Camarillo, CA). Antibody directed against the intracellular C-terminus of Kv1.2 (α-Kv1.2i) was purchased from Upstate Biotechnology (Lake Placid, NY). All other reagents were purchased from Sigma (St. Louis, MO) unless otherwise noted. pCB1 Dynamin K44A was a gift from Dr. Mark Caron. EGFP-N1 was purchased from Clontech (Palo Alto, CA). EGFP-Kvβ2 was a gift from Dr. Lilly Jan.

Tissue Culture

Human embryonic kidney 293 cells (HEK293 cells) stably expressing M1 mAChRs under G418 selection (Peralta *et al.*, 1988) were cotransfected with pCDNA3 plasmids containing the Kv1.2-α or Kvβ2 and a selectable marker for Zeocin (Tsai *et al.*, 1999). Clonal cell lines expressing M1 mAChRs, Kv1.2-α, and Kvβ2 were maintained in DMEM supplemented with 10% fetal bovine serum, 10 U/ml penicillin and streptomycin, and 2 mM L-glutamine and were under selected with 500 μg/ml G418 and 200 μg/ml Zeocin. Confluent cultures were plated to a density of 120×10^3 cells per cm^2 12 h before use onto noncoated tissue culture plates (Corning Glass Works, Corning, NY) for biochemistry, flow cytometry and electrophysiology experiments and onto noncoated glass cover slips (Corning Glass Works) for immunofluoresence experiments.

Transient Transfection of HEK Cells and Neurons

HEK293 cells were transiently transfected with pCMV-Kv1.2 alpha subunit and EGFP-Kvβ2 beta subunit using the TransIT-293 liposomal transfection reagent (Mirus, Madison, WI) as per the supplied protocol. Hippocampal neurons were transfected using Lipofectamine 2000 (Invitrogen, Carlsbad, CA) according to the supplied protocol.

Detection of Surface Kv1.2 Levels

For flow cytometric detection of surface Kv1.2, HEK293 cells stably expressing Kv1.2 were treated with a saline control solution or an appropriate stimulus and then metabolically poisoned with a solution of 154 mM sodium azide in PBS at 37°C for 10 min. This method blocks receptor-mediated endocytosis of transferrin receptors in HeLa and K562 cells by blocking ATP production (Schmid and Carter, 1990). We have found that this procedure also eliminates stimulus-induced Kv1.2 endocytosis in HEK293 cells, presumably by the same mechanism of ATP depletion. We also observe that, unlike fixation with formaldehyde, azide treatment does not permeabilized HEK293 cells, making it a suitable means by which to terminate endocytosis before detection of surface Kv1.2. We prefer this method over cold temperature block of endocytosis for flow cytometry experiments because azide-treated cells are more easily lifted and dissociated from one another.

For consistency, we also use azide treatment to terminate endocytosis in experiments that do not involve flow cytometry. After azide treatment, the cells are lifted and placed in a test tube where Kv1.2 remaining on the cell surface is labeled with a rabbit polyclonal antibody (α-Kv1.2e) directed against an extracellular epitope within the first intrahelical extracellular loop of the channel (Biosource International). Depending on the experiment, that antibody was labeled with a fluorescently labeled Fab fragment of a goat anti-rabbit antibody of using the Zenon antibody labeling kit (Molecular Probes, Eugene, OR) before application to live cells or was labeled with a fluorescently conjugated anti-rabbit IgG after the cells had been azide treated. The cells were then washed, and fluorescence was detected by flow cytometry as described below. For biochemical detection of surface Kv1.2 levels, antibody bound to surface channel was recovered by immunoprecipitation: cells were lysed in RIPA buffer (50 mM Tris, 150 mM NaCl, 1 mM EDTA, 0.1% deoxycholate, 1% NP-40, 10% glycerol, 1 mM DTT, 1 mM NaF, 1 mM NaOrthovanadate, protease inhibitor cocktail [Sigma], pH 8.0), the lysate was cleared by centrifugation at $22{,}000 \times g$ for 4 min and the Kv1.2-antibody complex was collected onto protein G-conjugated beads (Zymed, South San Francisco, CA). The beads were washed and the immunoprecipitated Kv1.2 protein was detected and quantified by Western blot probed with a monoclonal anti-Kv1.2 antibody (Upstate Biotechnology) followed by secondary antibody conjugated to a fluorescent fluorophore. Signal intensity was quantified using the Odyssey imaging system (Li-Cor, Lincoln, NE). For immunofluoresence detection of surface Kv1.2, cells were labeled with α-Kv1.2e as described above, followed by fixation and imaging as described below. In most cases the cells were labeled with intact α-Kv1.2e that had been previously labeled with a fluorescent Fab fragment of anti-rabbit IgG. However, in some cases Fab fragments of α-Kv1.2e were generated by papain digestion using a kit from Pierce (Rockford, IL).

Detection of Kv1.2 Endocytosis in HEK Cells

Surface Kv1.2 on live HEK293 cells was labeled (10 min, 37°C) with anti-Kv1.2 antibody that had been previously labeled with a fluorescently labeled Fab fragment of a goat anti-rabbit antibody of using the Zenon antibody labeling kit (Molecular Probes). This method of labeling live cells avoids clusterin-induced endocytosis often caused by IgG cross-linking. The cells were then washed once with growth medium at 37°C and then treated with the appropriate stimulus. Endocytosis was then terminated by addition of 154 mM sodium azide for 10 min at 37°C. Antibody remaining on the cell surface was next removed by acid wash (0.5 M NaCl/0.2 M acetic acid, 4 min, 0°C; Zhou *et al.*, 1995; Wilde *et al.*, 1999). Internalized fluorescence was then detected by flow cytometry as described below. For detection of channel internalization by immunofluoresence microscopy, azide-treated cells were transferred to an ice bath and acid washed before further processing.

Detection of Kv1.2 endocytosis in hippocampal neurons

Hippocampal neurons harvested from E18 rat embryos were transfected at 7 d in vitro with a mammalian expression vector harboring the gene for Kv1.2. Seven days after transfection, surface Kv1.2 was labeled in live cells using fluorescently tagged α-Kv1.2e antibody as described for HEK293 cells above. The cells were then treated with either a saline control solution or with 100 μM glutamate for 10 min after which they were washed and processed for immunofluoresence exactly as described above for HEK293 cells. Kv1.2 localization to the cell periphery or intracellular vesicles was detected using the DeltaVision deconvolution restoration microscopy system (Applied Precision, Issaquah, WA).

Flow Cytometry

A single laser flow cytometer (Epics XL; Coulter, Hialeah, FL) was used to quantify fluorescence signal. In nontransfected cells, α-Kv1.2e primary antibody was detected by labeling with Alexa-488–conjugated goat α-rabbit secondary antibody. Control experiments using this secondary but not primary antibody were performed for each experiment to determine background staining. In cells transfected with GFP (excitation peak = 488 nm, emission

peak = 508 nm), α-Kv1.2e primary antibody was labeled with a goat α-rabbit secondary antibody conjugated to PE/Cy™5 with an excitation peak of 488 nm and an emission peak of 667 nM (Southern Biotechnology, Birmingham, AL). Surface Kv1.2 in transfected cells was taken as the distribution of cells emitting at 667 nm in cells (indicating surface Kv1.2) and also emitting at 488 nm (indicating GFP expression). In these experiments, controls using goat α-rabbit-PE/Cy5 without prior application of primary antibody were performed to determine background staining. Detection of surface Kv1.2 was accomplished by applying primary and secondary antibodies after the cells had been drug and azide-treated. Detection of internalized Kv1.2 was accomplished by permeabilized drug and azide-treated cells with 0.1% Triton X-100 before application of secondary antibody.

Immunofluoresence

Cells were grown on glass cover slips exactly as cells grown directly on 35-mm plates. After appropriate treatment as described above, the cells were fixed with 4% formaldehyde (Polysciences, Warrington, PA) in PHEM 6.1 buffer (60 mM PIPES, 25 mM HEPES, 2 mM $MgCl_2$, 10 mM EGTA; pH to 6.1 with KOH; Schliwa *et al.*, 1981) for 20 min at room temperature followed by a wash. The plates were then placed on ice, and the cells were extracted with ice cold acetone for 4 min. After washing with PHEM buffer at pH 6.9, the cells incubated in blocking buffer (PHEM 6.9, 3% goat serum, 10 μg goat IgG, 0.1% fish skin gelatin) for 1 h at room temperature. They were then treated with primary antibody (Kv1.2e = 1.1 μg/μl, EEA1 = 1.25 μg/μl) diluted in blocking buffer. After a subsequent wash (three times for 5 min in PHEM 6.9) they were treated with secondary antibody (4 μg/μl in blocking buffer) for 1 h at room temperature. After wash the slides were mounted on glass slides with ProLong mounting medium (Molecular Probes) according to instructions. Imaging was with the DeltaVision reconstruction microscopy system (Applied Precision).

Electrophysiology

All recordings were made using the whole cell patch clamp method. Data were collected using an Axopatch 200 patch-clamp amplifier using pClamp 8 (Axon Instruments, Burlingame, CA). All traces were leak subtracted using a P/4 protocol from a holding potential of −60 mV. The pipette solution contained 60 mM K_2SO_4, 1.2 mM KCl, 5 mM $MgSO_4$, 5 mM Na^+-HEPES, and 35 mM sucrose (pH 7.1). The external (bath) solution contained 118 mM NaCl, 2.5 mM KCl, 1.8 mM $CaCl_2$, 0.8 mM $MgCl_2$, 5 mM Na^+-HEPES, and 23 mM glucose (pH 7.4). All recordings were made at 37°C.

Statistical Methods

The Mann-Whitney *U* test was used to derive p values to determine statistical significance of treatment effects.

RESULTS

Surface-expressed Kv1.2 Varies Independently of Total Channel Expression

The initial indication that the regulation of Kv1.2 ionic current involves trafficking of the channel protein from the plasma membrane arose from our observation that the amount of Kv1.2 detectable at the cell surface varies considerably in cells stably expressing constant levels of Kv1.2 protein. Surface Kv1.2 was labeled by application to live cells of a polyclonal antibody (α-Kv1.2e) directed toward an epitope within the first extracellular loop of Kv1.2 (aa192–208). Total Kv1.2 protein was labeled with a mAb directed against the C-terminus of Kv1.2 (α-Kv1.2i) applied after the same cells had been fixed and permeabilized (Figure 1A). The differential labeling of surface and internal Kv1.2 was confirmed in Figure 1B by colocalization α-Kv1.2e applied to the surface of live cells (green) with cortical F-actin labeled with fluorescent phalloidin (blue) and imaged as an optical slice through the horizontal plane of unstimulated cells. Colocalization with cortical actin was not observed with α-Kv1.2i applied after the same cell had been fixed and permeabilized (red). To confirm that application of antibody to the surface of live cells does not enter the cell and cannot therefore label intracellular Kv1.2, α-Kv1.2i was applied to the surface of live cells followed by fixation, permeabilization, and labeling with phalloidin and Alexa-568 goat anti-mouse secondary antibody (Figure 1C, left). No Alexa-568 signal (green) was observed, despite confirmation of cell permeabilization as evidenced by efficient labeling of F-actin with phalloidin (blue). Conversely, to demonstrate that surface applied α-Kv1.2e applied to permeabilized cells is capable of labeling total Kv1.2 rather than only surface channel, α-Kv1.2e was applied to fixed and permeabilized cells (Figure 1C, right). With this method of labeling, the pattern of Kv1.2 staining (green) resembles that of α-Kv1.2i applied to permeabilized cells in that staining exists throughout the cytoplasm and is not limited to the cortical actin-rich cell periphery (blue). Collectively, these findings confirm that application of α-Kv1.2e to the exterior of nonpermeabilized cells is an effective means of exclusively labeling Kv1.2 expressed at the cell surface. As expected for a clonal cell line, total Kv1.2 expression varied little between individual cells (Figure 1A, left). In contrast, Kv1.2 accessible to antibody applied to the cell surface varied considerably within the same population of cells (Figure 1A, right). Variability in surface Kv1.2 levels was particularly intriguing in view of the considerable variability evident in the amplitude of standing Kv1.2 ionic current measured in the same cell line; steady state Kv1.2 ionic current measured by whole cell patch clamp and evoked by depolarization to +40 mV had a mean amplitude of 1.7 nA, and an SD of 0.5 nA (n = 16). Taken together, these data led us to hypothesize that regulated trafficking of Kv1.2 from the cell surface may constitute a physical mechanism for the suppression of Kv1.2 ionic current by tyrosine phosphorylation.

That hypothesis predicts that stimuli capable of evoking channel tyrosine phosphorylation and suppression should also decrease the level of Kv1.2 at the cell surface. One such stimulus is the activation of M1 muscarinic acetylcholine receptors, also stably expressed in this cell line. We therefore measured the effect of M1 receptor activation on the surface expression of Kv1.2. Figure 1D reveals that M1 receptor activation 10 μM with carbachol (CCh) applied for 10 min had no effect on total Kv1.2 expression but strongly reduced Kv1.2 levels at the cell surface. Biochemical confirmation of this finding was demonstrated by immunoprecipitation and subsequent Western analysis of Kv1.2 accessible to α-Kv1.2e antibody applied to the surface of cells that had first been treated for 10 min with saline or with 10 μM carbachol (Figure 1E). Western analysis of the total lysate revealed that carbachol had no effect on the overall level of Kv1.2 expression. The bar graph summarizes densitometry data from 13 experiments. The asterisk denotes a significant carbachol induced loss of surface Kv1.2 ($p < 0.007$). To further quantify the effect of carbachol stimulation on Kv1.2 surface expression, we used flow cytometry to detect fluorescently tagged α-Kv1.2e bound to surface Kv1.2 in intact cells (Figure 1F). The top panel shows representative distributions of fluorescence intensity for unlabeled (black), labeled and untreated (white), and labeled and carbachol-treated cells. The bottom panel summarizes data from 11 individual experiments. Histograms represent the mean cell count normalized to the saline control. The asterisk indicates a significant carbachol induced shift in the distribution of cells toward lower levels of Kv1.2 surface expression ($p < 0.0001$). Collectively, the data in Figure 1 demonstrate that activation of M1 muscarinic receptors, a stimulus know to induce the tyrosine phosphorylation-dependent suppression of Kv1.2 ionic current, also induces a significant loss of Kv1.2 from the cell surface without affecting total Kv1.2 expression levels within the cell.

To further correlate loss of surface Kv1.2 with channel suppression, we asked whether loss of surface channels could be evoked by other stimuli known to cause tyrosine phosphorylation-dependent channel suppression. Such

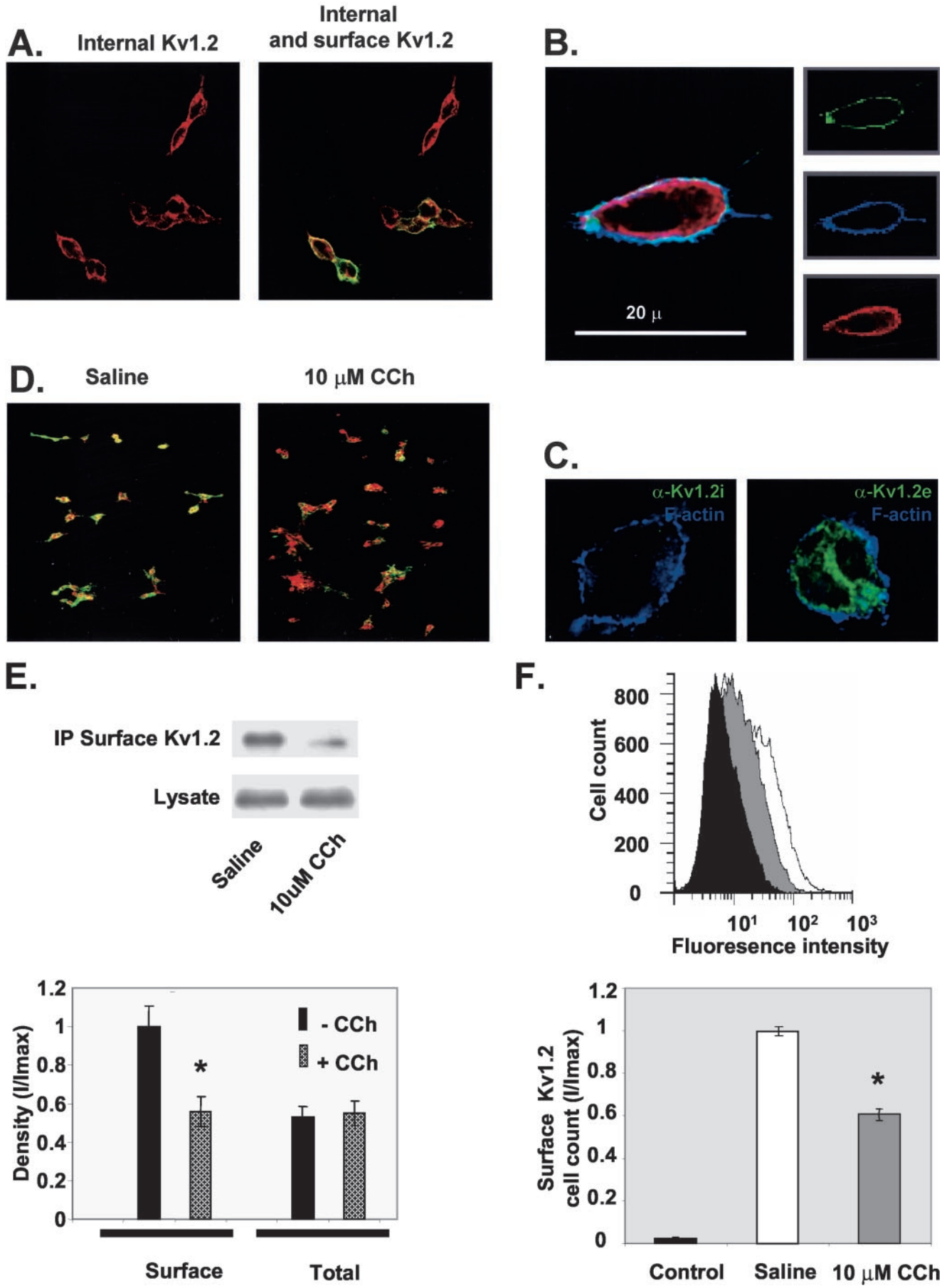
A.
Internal Kv1.2
Internal and surface Kv1.2
B.
20 μ
D.
Saline
10 μM CCh
C.
α-Kv1.2i
F-actin
α-Kv1.2e
F-actin
E.
IP Surface Kv1.2
Lysate
Saline
10uM CCh
F.
Cell count
800
600
400
200
0
10¹
10²
10³
Fluoresence intensity
Density (I/Imax)
1.2
1
0.8
0.6
0.4
0.2
0
- CCh
+ CCh
*
Surface
Total
Surface Kv1.2 cell count (I/Imax)
1.2
1
0.8
0.6
0.4
0.2
0
*
Control
Saline
10 μM CCh

Figure 1.

agents include the tyrosine phosphatase inhibitor pervanadate (Tsai *et al.*, 1999) as well as the calcium ionophore ionomycin and the PKC activator PMA (Huang *et al.*, 1993). We found that, in addition to carbachol, pervanadate (32 μM/10 min), ionomycin (1 μM/10 min), and PMA (100 nM/10 min) all caused a significant loss of surface Kv1.2 as measured by flow cytometry (Figure 2). Each histogram represents the average of at least five individual experiments. The error bars represent the SE of the mean (SEM). Therefore, loss of Kv1.2 is caused by a variety of stimuli capable of triggering tyrosine phosphorylation-dependent channel suppression, further supporting a role for the regulation of surface Kv1.2 levels in channel suppression.

Endocytosis Is a Mechanism for Stimulus-induced Loss of Surface Kv1.2

An increasingly large body of evidence now exists indicating a role for the actin cytoskeleton in the endocytosis of plasma membrane proteins (Jeng and Welch, 2001). One of the actin-binding proteins recently found to contribute to some forms of endocytosis is cortactin (Olazabal and Machesky, 2001; Cao *et al.*, 2003). Because cortactin has a role in Kv1.2 regulation (Hattan *et al.*, 2002), we explored the possibility that stimulus-induced loss of surface Kv1.2 occurs through endocytosis. To test this idea, surface-expressed Kv1.2 was labeled with fluorescently tagged α-Kv1.2e antibody and the cells were then stimulated with either CCh (10 μM, 10 min) or pervanadate (32 μM, 10 min) to induce loss of surface channel. Antibody bound to Kv1.2 remaining on the cell surface was removed by acid wash (Zhou *et al.*, 1995; Wilde *et al.*, 1999), and further processing of the internalized protein was stopped by fixing the cells with 4% formaldehyde. In this way endocytosed Kv1.2 can be detected as an increase in fluorescence within the cell. Using the DeltaVision deconvolution fluorescence microscopy system (Applied Precision) to generate optical sections, we found that treatment with pervanadate produced a strong increase in internalized α-Kv1.2e compared with controls (Figure 3). The left-most panels show a compression of all Z-sections taken through the cells before or after treatment with pervanadate (Figure 3, A and C, respectively). Importantly, a single 0.2-μm-thick optical section through the center of the cells (Figure 3, B and D) reveals that much of the internalized channel lies adjacent to the plasma membrane in small, clearly distinguishable vesicles. Such Kv1.2 internalization was quantified by flow cytometry (Figure 3E), revealing a significant increase in fluorescence in pervanadate-treated cells compared with cells treated with saline alone ($p < 0.05$, $n = 5$). Similar results were obtained with cells treated with carbachol ($p < 0.006$, $n = 5$). Stimulus-induced increase in fluorescence was the result of Kv1.2 internalization and was not caused by nonspecific endocytosis or pinocytosis of nonspecifically bound antibody because no significant fluorescence increase was detected in an identical set of experiments done with the parental HEK293 cell line lacking Kv1.2 (Figure 3F). Some internalized label is evident in nonstimulated cells, possibly resulting from a low level of basal endocytosis. To do test that idea, surface Kv1.2 was labeled in cells that had been first treated with sodium azide to block endocytosis. Comparison of control vs. acid-washed cells so labeled revealed that acid wash eliminates virtually all Kv1.2 surface labeling (Figure 3C), considerably more than that removed by acid wash of live-labeled cells, suggesting that internalized fluorescence seen in live, saline-treated cells resulted from a low level of basal endocytosis.

To confirm that stimulus-induced endocytosis was not caused by channel clustering induced by application of the primary antibody, we compared the effect of labeling live cells with either α-Kv1.2e IgG or α-Kv1.2e Fab fragment. In

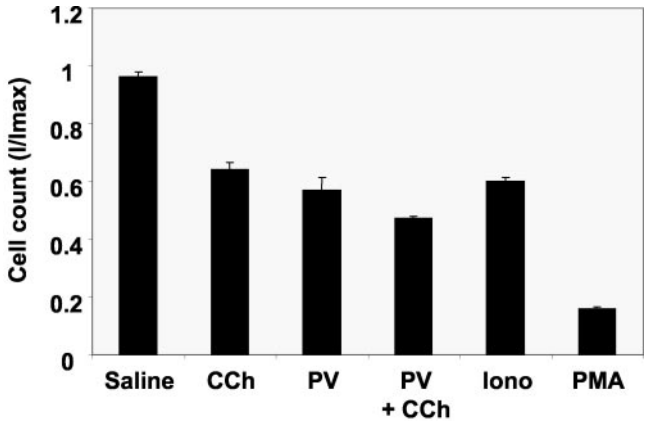

Figure 2. Stimuli that induce tyrosine kinase-dependent suppression of Kv1.2 also induce loss of surface Kv1.2. The average level of surface Kv1.2 expression was measured by flow cytometry of cells labeled with a fluorescently tagged antibody directed against an extracellular epitope of Kv1.2. Cells were treated with saline, carbachol (10 μM), pervanadate (32 μM), carbachol + pervanadate, ionomycin (1 μM), or PMA (100 nM) for 10 min before labeling Kv1.2 remaining on the cell surface. Histograms represent the means normalized to the saline control. All treatments caused a significant loss of surface Kv1.2 ($p < 0.0001$).

Figure 1 (facing page). Regulated surface expression of Kv1.2. (A) Surface expression of Kv1.2 was compared with total Kv1.2 levels in cells stably expressing Kv1.2. Left, total Kv1.2 labeled with a mouse mAb (α-Kv1.2i) after cell fixation and permeabilization; right, surface Kv1.2 labeled with a rabbit polyclonal antibody that recognizes an extracellular epitope within the channel (α-Kv1.2e) applied to live cells before fixation. (B) Differential subcellular localization of surface vs. total Kv1.2. Left, a horizontal optical slice through a cell labeled with α-Kv1.2e before permeabilization (green), followed by labeling with α-Kv1.2i (red) and Alexa-488 phalloidin after fixation and permeabilization (blue). Right, separate images of each optical channel. (C) Antibody application method dependent labeling of surface vs. intracellular Kv1.2. Left, lack of Kv1.2 labeling of live cells treated with α-Kv1.2i mouse mAb before fixation is shown. F-actin was labeled with Alexa-488 phalloidin (blue) and Alexa-568 goat anti-mouse secondary antibody (green) after the cells had been fixed and permeabilized. Right, α-Kv1.2e (green) is capable of labeling total, rather than only surface Kv1.2 when applied to fixed and permeabilized cells. F-actin was labeled with Alexa-488 phalloidin (blue). (D) Cells labeled for total and surface Kv1.2 subsequent to treatment with saline (left panel) or 10 μM carbachol (right panel) reveal carbachol induced loss of surface Kv1.2. (E) Top panel, a Western blot of surface Kv1.2 immunoprecipitated from cells that had previously been treated with saline or carbachol. Western blot of the lysate from the same cells reveals that the total Kv1.2 levels are unaffected by carbachol; bottom panel, a summary of densitometry readings from 13 similar experiments; histograms depict the mean ± the SE of the mean (SEM). Asterisk denotes significant change from control ($p < 0.007$). (F) Top panel, histograms of surface Kv1.2 measured by detection flow cytometry. The distribution of unlabeled cells is shown in black. The distributions for cells in which surface Kv1.2 had been labeled with a fluorescent antibody after treatment with saline or carbachol are shown in white and gray, respectively. The bottom histogram represents summary data from nine individual flow cytometry experiments and depicts mean fluorescent cell count normalized to saline-treated controls ± SEM. As denoted by the asterisk, carbachol caused a significant loss of surface Kv1.2 fluorescence relative to control ($p < 0.0001$).

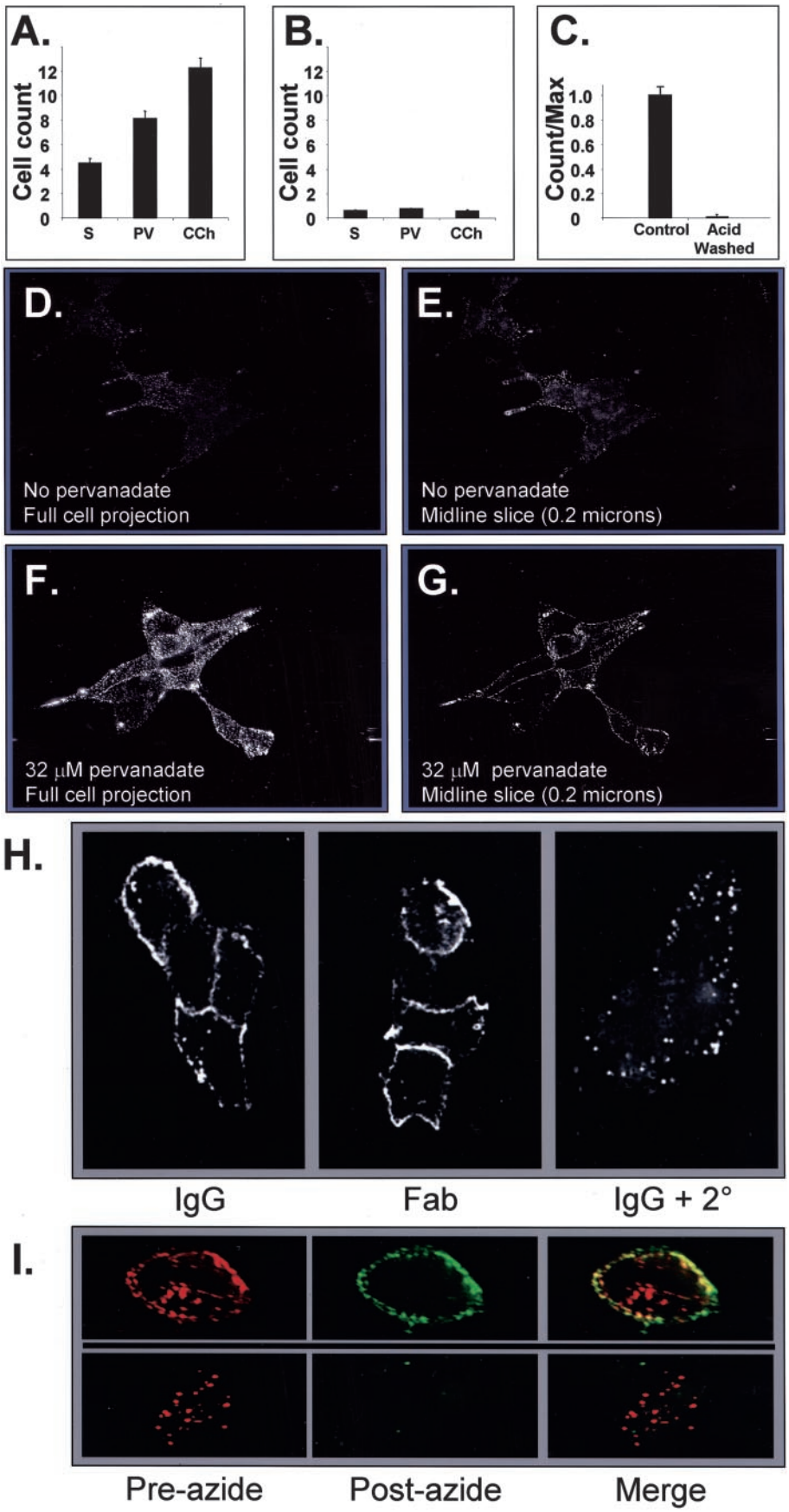

Figure 3. Loss of surface Kv1.2 is caused by endocytosis. (A) Cells in which surface Kv1.2 has first been labeled with fluorescently tagged anti-Kv1.2 antibody were treated with saline, carbachol (10 μM), or pervanadate (32 μM) for 10 min followed by acid was to remove remaining surface antibody. Internalized Kv1.2 was detected as an increase in fluorescence measured by flow cytometry. Histograms summarize a minimum of five experiments ± SEM. Both pervanadate ($p < 0.05$, $n = 5$) and carbachol ($p < 0.005$, $n = 5$) caused a significant internalization of fluorescently tagged surface Kv1.2. (B) The same experiment depicted in A was done in cells not expressing Kv1.2. No significant stimulus-induced increase in fluorescence was detected in these control cells, indicating that the signal shown in A is specific to Kv1.2. (C) Comparison of nonacid wash vs. acid-washed cells in which endocytosis had been blocked by pretreatment with sodium azide reveals that acid wash removes >98% of antibody bound to surface Kv1.2. (D-G) Immunofluorescence detection of internalized Kv1.2 in saline-treated cells (D and E) or cells treated with pervanadate (F and G) reveals that cell stimulation causes internalization of Kv1.2 into vesicular compartments. (H) Surface labeling of live cells with fluorescently tagged intact α-Kv1.2e IgG (left) or a Fab fragment of the same antibody (middle) fails to induce Kv1.2 internalization. In a positive control for clustering-induced channel internalization, α-rabbit IgG was applied to live cells secondary to labeling with α-Kv1.2e (right). (I) Non-overlap of surface vs. internalized Kv1.2 labeled with α-Kv1.2e demonstrated by sequential application of differentially labeled secondary Fab fragments before (red) and after azide block of PMA (100 nM)-induced endocytosis (green). Top, a cell with incomplete PMA induced endocytosis; bottom, a cell from the same coverslip with complete PMA induced channel internalization.

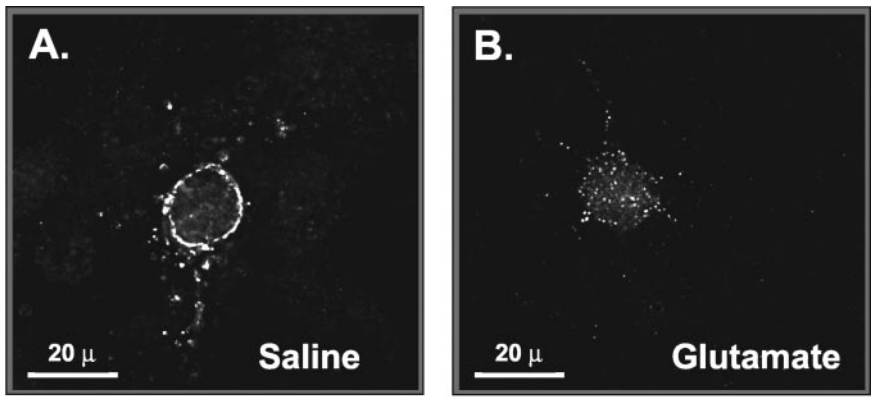

Figure 4. Endocytosis of Kv1.2 in rat hippocampal neurons. (A) Surface-expressed Kv1.2 in mature hippocampal neurons (14 days in vitro) was labeled with a fluorescence labeled antibody and then treated with saline for 10 min. An optical slice through the cell center reveals that Kv1.2 is localized to the periphery in these cells. (B) An optical slice through the center of similarly labeled cells treated with glutamate (100 μM) for 10 min reveals redistribution of Kv1.2 into small vesicular compartments in response to glutamate.

neither case did we observe a difference in the quality of staining (Figure 3H, left and middle panels). In contrast, application of an intact α-rabbit IgG to the surface of live cells that had first been labeled with α-Kv1.2e did induced channel internalization (Figure 3H, right panel). Therefore, although Kv1.2 is susceptible to antibody-mediated, clustering-induced endocytosis, labeling with intact α-Kv1.2e IgG does not itself induce channel internalization.

To further demonstrate that the puncta generated by drug stimulation represent internalized channel and not, for example, clustering of channel at the cell surface, we differentially labeled surface vs. internalized Kv1.2 with two different fluorophores, one during and the other after termination of endocytosis, and assessed the degree of signal overlap (Figure 3I). Surface Kv1.2 in live cells was labeled with Fab-GAR-Alexa-568 (red) before induction of endocytosis by application of 100 nM PMA. After 10 min, endocytosis was terminated by application of sodium azide. The cells were then labeled with Fab-GAR-Alexa-647 (green). The top panel of Figure 3I shows a cell in which both surface and punctuate Kv1.2 signal can be observed in the Alexa-568 channel (red), suggesting that endocytosis occurred but was not complete. Application of Fab-GAR-Alexa-657 (green) after endocytosis had been terminated is limited to the surface of the cell. Absolutely no overlap with the red puncta is observed, indicating that they were not accessible to surface applied secondary antibody. The bottom panel shows a nearby cell in which Fab-GAR-Alexa-647 applied as above produced no labeling, indicating that this cell had undergone nearly complete endocytosis of Kv1.2 from its surface. Thus, Kv1.2-positive puncta are not labeled after termination of endocytosis, indicating that those puncta represent internalized endosomal compartments.

Most of the studies reported here use Kv1.2 overexpressed in HEK293 cells, and questions can be raised as to the general relevance of those findings outside of that model system. The initial finding that Kv1.2 undergoes tyrosine phosphorylation-induced suppression was made using the *Xenopus* oocytes expression system (Huang *et al.*, 1993), indicating the phenomenon occurs in diverse model systems. Further, subsequent work suggests a role for tyrosine phosphorylation-dependent regulation of Kv1.2 as well as other Kv1 family channels, in a variety of intact organ systems, heart (Sah *et al.*, 1999), and brain (Fadool *et al.*, 2000; Lambe and Aghajanian, 2001; Qiu *et al.*, 2003; Colley *et al.*, 2004). Thus, given that the phenomenon of Kv1 family channel suppression occurs in a range of model systems and given that such suppression has more recently been identified in intact organs, we believe that the use of HEK293 cells to investigate the molecular mechanisms involved in that suppression is well supported. Nevertheless, it is important to confirm that our findings in HEK293 cells extend to cells in which Kv1.2 is thought to have a natural role. To do so, we asked whether stimulus-induced channel endocytosis could be detected in primary culture hippocampal neurons. Surface Kv1.2 expressed in hippocampal neurons (nonacid washed) was labeled with fluorescently tagged α-Kv1.2e antibody. An optical slice through the cell center reveals peripheral staining of Kv1.2 in a saline-treated control cell (Figure 4A). In contrast, an optical slice through the center of a cell that had been treated with glutamate (100 μM, 10 min) after having been first labeled for surface Kv1.2 reveals that stimulation of glutamate receptors causes a profound translocation of Kv1.2 from the cell surface into intracellular vesicles (Figure 4B). These results support the idea that analysis of Kv1.2 endocytosis in HEK293 cells provides insight into channel regulation in more natural systems.

Endocytosis proceeds through a variety of mechanisms; however, a common pathway involves movement of membrane proteins into early endosomes, structures that are defined in part by the presence of the protein EEA1 (Mu *et al.*, 1995). We therefore asked whether internalized Kv1.2 colocalizes with EEA1. Surface Kv1.2 labeled with α-Kv1.2e antibody is retained at the cell surface after treatment with a control saline solution (Figure 5A). Early endosomes stained with EEA1 appear as discrete intracellular puncta. Neither the Kv1.2 nor EEA1 signals show significant overlap in control cells. In contrast, activation of M1 receptors with carbachol causes translocation of surface Kv1.2 into intracellular puncta (Figure 5B). Importantly, those puncta exhibit a striking colocalization with EEA1.

We note that in some cases, including those shown here, M1 receptor activation causes a reorganization of the cytoarchitecture resulting in a change in cellular morphology. This process appears to be distinct from Kv1.2 endocytosis because the change in cellular morphology does not occur in all carbachol-treated cells (unpublished data), or in cells treated with pervanadate (Figure 3). To confirm that idea, live cells were surface-labeled with α-Kv1.2e and treated with either saline or PMA (100 nM, 10 min), fixed, permeabilized, and stained with α-EEA1 to label early endosomes and with fluorescently labeled phalloidin to label F-actin. Surface Kv1.2 in untreated cells exhibits a striking colocalization with F-actin, and lack of colocalization with early endosomes (Figure 5C, top panels). In contrast, treatment with PMA induced a profound internalization of Kv1.2 and concomitant colocalization with early endosomes (Figure 5C, bottom panels). However, in contrast to carbachol-treated cells, PMA did not cause a change in cellular morphology. Indeed, F-actin labeling appears unchanged in sa-

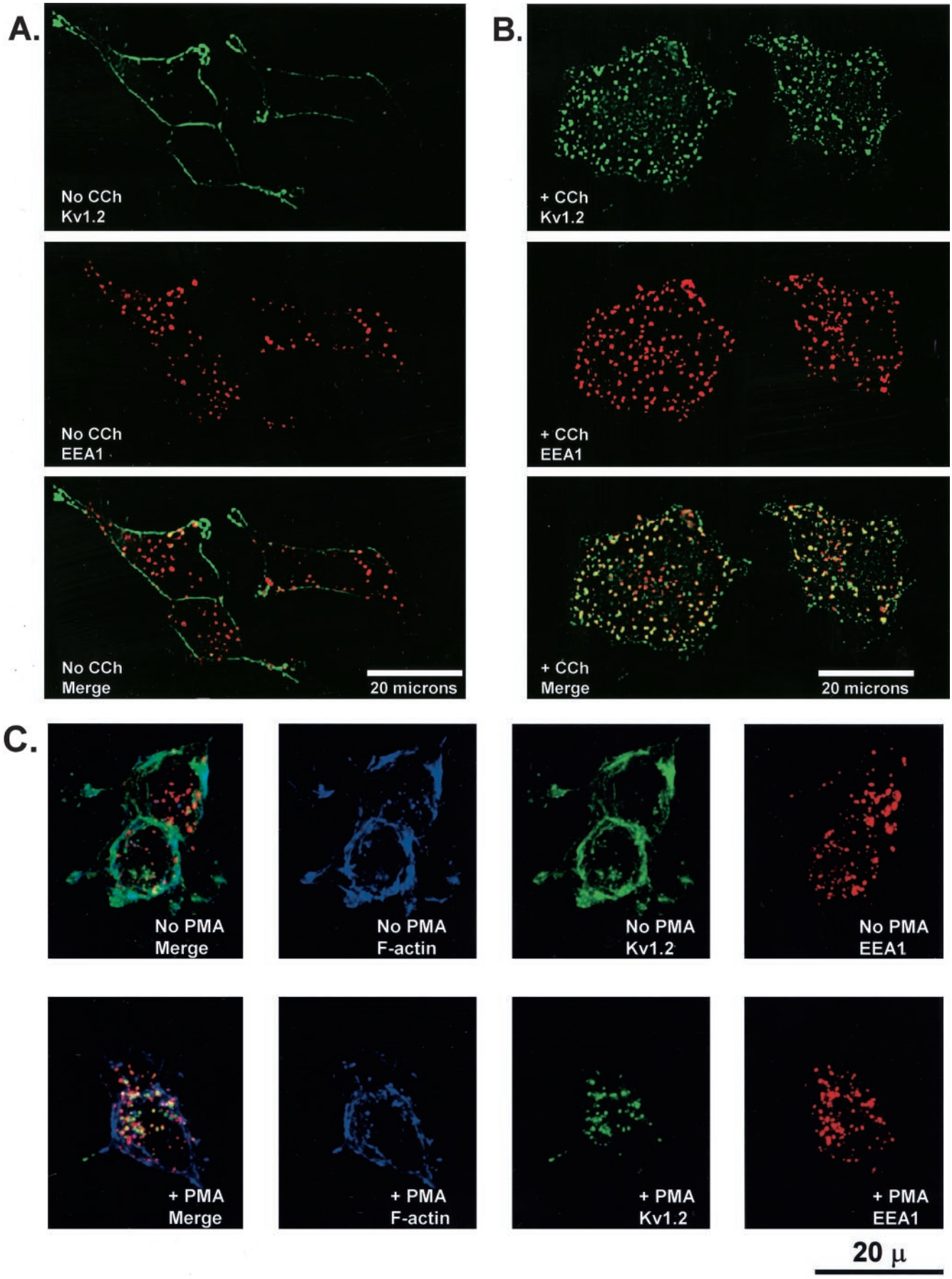
A.
No CCh
Kv1.2
No CCh
EEA1
No CCh
Merge
20 microns
B.
+ CCh
Kv1.2
+ CCh
EEA1
+ CCh
Merge
20 microns
C.
No PMA
Merge
No PMA
F-actin
No PMA
Kv1.2
No PMA
EEA1
+ PMA
Merge
+ PMA
F-actin
+ PMA
Kv1.2
+ PMA
EEA1
20 μ

Figure 5.

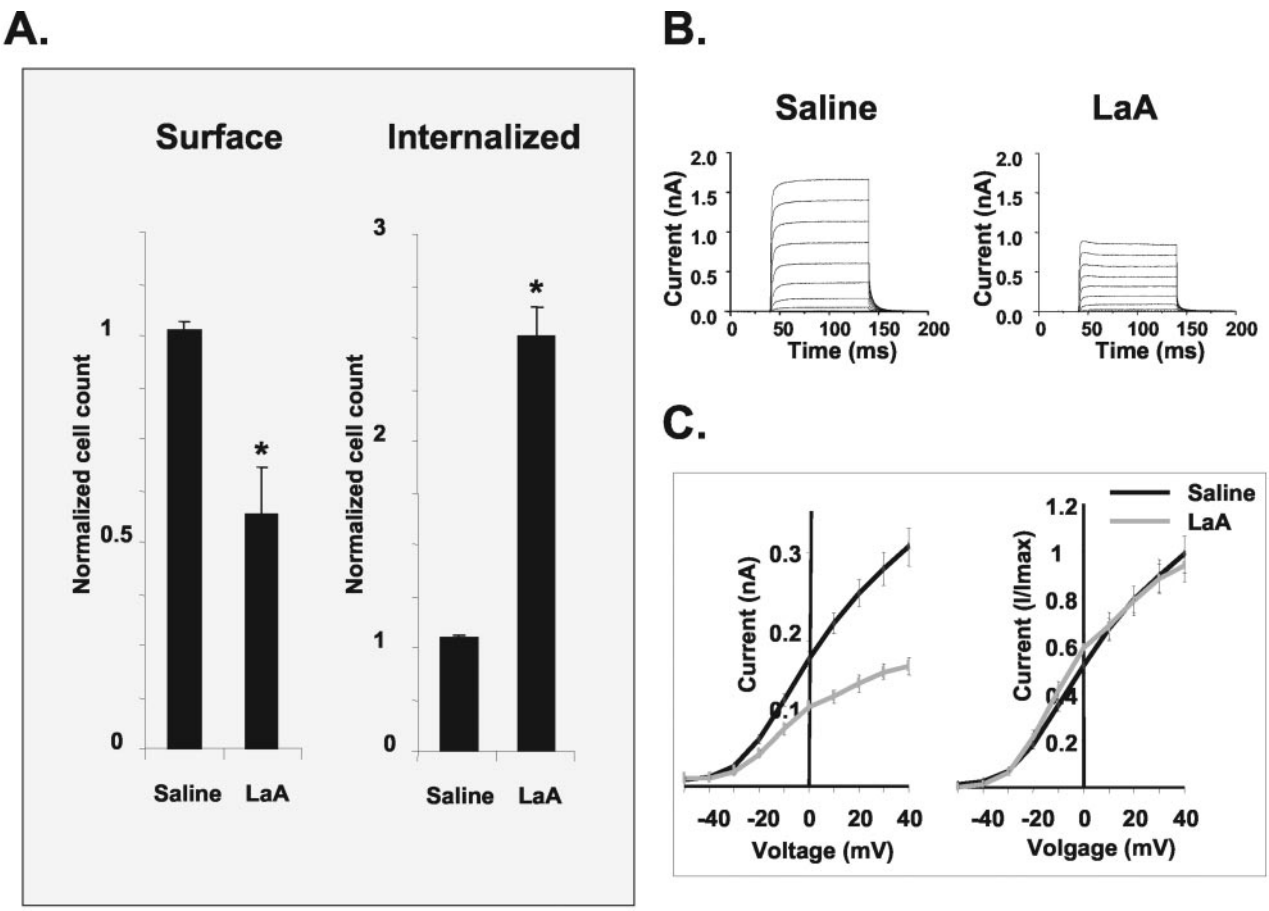

Figure 6. Disruption of the actin cytoskeleton causes endocytosis of Kv1.2 and suppression of Kv1.2 ionic current. (A) Flow cytometric detection of surface Kv1.2 labeled after treatment with 9.4 μM latrunculin A (LaA) for 30 min reveals that such treatment causes a significant ($p < 0.002$) loss of surface Kv1.2 (left). Loss of surface Kv1.2 was caused by channel endocytosis because the same treatment caused a significant increase in internalized Kv1.2. Surface Kv1.2 was labeled with fluorescently tagged antibody before LaA treatment and noninternalized antibody was removed by acid wash. Internalized fluorescence was detected by flow cytometry. Asterisk indicates a significant ($p < 0.004$) increase in internalized Kv1.2 in LaA-treated cells. (B) Ionic current is significantly reduced after treatment with LaA (9.4 μM, 30 min). Steady state current amplitude evoked from each cell was measured for analysis, (mean at + 40 mM = 1.7 nA (control) vs. 0.9 nA (LaA), $p < 0.0001$). Graphic representation of latrunculin effects are depicted by current traces representing the numerical average of individual ionic current traces evoked from at least 14 cells. Trace averages were generated using the AxoClamp software. (C) Tail current amplitudes of the cells depicted in B were plotted against the step voltage amplitude to generate activation curves (left). Normalization of both curves to their respective peak value reveals identical voltage dependence of the current generated in saline vs. LaA-treated cells (right).

line- vs. PMA-treated cells, confirming that internalization of Kv1.2 does not require a gross rearrangement of the actin cytoskeleton.

Figure 5 (facing page). Stimulus induced entry of Kv1.2 into early endosomes. (A) Surface Kv1.2 was labeled with α-Kv1.2e before treatment of the cells with a saline control solution. The cells were fixed and endosomes were labeled with an mAb directed against EEA1, an early endosome marker protein. Fluorescence-conjugated secondary α-rabbit or anti-mouse antibodies were used to tag the α-Kv1.2e (green) or α-EEA1 (red) antibodies, respectively. Most Kv1.2 signal is evenly distributed at the cell surface and does not overlap with the punctuate EEA1 signal. (B) After treatment with carbachol (10 μM, 10 min), Kv1.2 redistributes to intracellular puncta determined to be early endosomes by positive staining for the early endosomal marker protein EEA1. (C) Entry of Kv1.2 into early endosomes does not require gross restructuring of the actin cytoskeleton. Surface labeled Kv1.2 in cells treated with saline (top) or with 100 nM PMA (bottom) is depicted in green. Phalloidin-labeled F-actin (blue) and EEA1 (red) were labeled after the cells were fixed and permeabilized.

A Role for Actin in Kv1.2 Endocytosis

The lack of gross rearrangement of the actin cytoskeleton observed in Figure 5 does not indicate that regulated actin dynamics is not involved in Kv1.2 endocytosis, but only that stimulus-induced endocytosis does not require a global alteration of the cytoarchitecture. Indeed, several lines of evidence suggest an important role for actin dynamics in Kv1.2 regulation. Previous studies have identified two actin-regulating proteins, RhoA (Cachero *et al.*, 1998) and cortactin (Hattan *et al.*, 2002), as having key roles in Kv1.2 regulation by tyrosine kinases. Other studies have shown that the actin cytoskeleton has a complex, albeit still poorly understood role in several types of endocytosis (Jeng and Welch, 2001; Qualmann and Kessels, 2002; Schafer, 2002). Together, these findings led us to hypothesize that the actin cytoskeleton may be involved in Kv1.2 endocytosis. To test this idea, we compared the effect of F-actin disruption on both Kv1.2 endocytosis and on Kv1.2 ionic current. To do so, we used latrunculin A, a toxin that binds to monomeric actin, preventing its incorporation into F-actin, thereby disrupting the

actin cytoarchitecture (Spector *et al.*, 1989). The left panel of Figure 6A shows that application of 9.4 μM latrunculin-A for 30 min caused a significant decrease in surface Kv1.2 levels. The acid wash experiments shown in the right panel of Figure 6A confirms that this results from latrunculin A-induced endocytosis of Kv1.2. If our model that Kv1.2 suppression is caused by channel endocytosis is correct, latrunculin A should therefore also cause a significant suppression of Kv1.2 ionic current. Indeed, Figure 6B shows this to be the case. The top panels show the averaged current traces of at least 14 cells treated with a control saline solution or with 9.4 μM latrunculin A. Figure 6C depicts activation curves of the tail current amplitudes measured after the depolarizing voltage step plotted against the step voltage amplitude. The left panel shows the tail current amplitudes for saline vs. latrunculin A-treated cells. The right panel shows the same data after normalization of both to the current amplitude at +40 mV. The overlap of each normalized activation curve demonstrates that, as is the case with M1 receptor-induced channel suppression, latrunculin A-induced suppression of Kv1.2 ionic current did not result from a shift in the channel's voltage dependence. These findings support the hypothesis that the actin cytoskeleton has a role in Kv1.2 regulation and in particular suggests a possible mechanism for Kv1.2 regulation in which F-actin serves to stabilize Kv1.2 on the cell surface.

Kv1.2 Tyrosine Y132 Is Required for Channel Suppression and Endocytosis

To establish a more direct relationship between tyrosine phosphorylation-dependent channel suppression and loss of surface Kv1.2 protein, we asked whether a mutation within Kv1.2 that inhibits channel suppression also inhibits channel endocytosis. Mutation of the N-terminal tyrosine Y132 to phenylalanine (Y132F), inhibits tyrosine phosphorylation-dependent Kv1.2 suppression (Huang *et al.*, 1993). If channel suppression is caused by loss of Kv1.2 from the cell surface, Y132F channels should also be resistant to stimulus-mediated endocytosis

Published experiments showing that channels harboring the Y132F mutation resist tyrosine phosphorylation-dependent channel suppression were performed using the *Xenopus* oocytes expression system (Huang *et al.*, 1993). It was therefore important to first confirm that Kv1.2-Y132F channels are also resistant to suppression when expressed in HEK293 cells. Figure 7A shows that ionic current generated by wild-type Kv1.2 expressed in HEK293 is suppressed upon activation of coexpressed M1 receptors, whereas, in contrast, M1 receptor activation has no significant effect on ionic current generated by similarly expressed Kv1.2-Y132F channels. In a parallel set of experiments measuring not ionic current but surface expression levels of Kv1.2 protein (Figure 7B), M1 receptor activation induced a significant loss of Kv1.2wt channel protein from the cell surface ($p < 0.006$, $n = 5$) but had no significant effect on Kv1.2-Y132F surface expression ($p > 0.1$, $n = 9$). Identical results were obtained with pervanadate.

Consistent with the above findings is our observation that, in contrast to wild-type Kv1.2 channels, stimulation with either pervanadate or carbachol fails to induce the colocalization of Kv1.2Y132F channels with early endosomes (Figure 7, C-F). Thus, a point mutation within Kv1.2 that confers resistance to stimulus-induced channel suppression also confers resistance to stimulus-induced trafficking of Kv1.2 from the cell surface, providing a key link between stimulus-induced Kv1.2 suppression and endocytosis.

It is possible that the negative result obtained above using a cell line stably expressing Kv1.2-Y132F channels arose not from a reduced ability of Kv1.2-Y132F channels to undergo endocytosis but from a signaling defect specific to the cell line itself. To control for this, we used immunoprecipitation of surface channel as a way to biochemically assay trafficking from the plasma membrane of transiently expressed channels. Here, Kv1.2wt, and Kv1.2-Y132F channels were transiently transfected into the same passages of HEK293 cells and subject to parallel experimental analysis. The cells were treated with a saline control or pervanadate (32 μM) for 10 min before termination of endocytosis with sodium azide. The Kv1.2 channel remaining on the cell surface was labeled with α-Kv1.2e, collected by immunoprecipitation, and detected by Western blot. As shown in Figure 7G, pervanadate caused a significant loss of Kv1.2wt channels from the cell surface ($p < 0.01$, $n = 8$). In contrast, pervanadate caused no significant change in the amount of Kv1.2-Y132F channels immunoprecipitated from the cell surface ($p > 0.4$, $n = 7$). Therefore, the differential behavior of Kv1.2-Y132F relative to Kv1.2wt likely arises from the point mutation itself and not from a systematic difference between Kv1.2-wt and Kv1.2-Y132F cell lines.

Taken together, these data demonstrate that the Y132F point mutation previously shown to affect Kv1.2 suppression in *Xenopus* oocytes also reduces Kv1.2 suppression in HEK 293 cells and has a parallel attenuating effect on Kv1.2 endocytosis, as measured by flow-cytometry, immunofluoresence, and immunoprecipitation.

Figure 7 (facing page). A mutation within Kv1.2 (Y132F) that confers resistance to ionic current suppression also blocks channel endocytosis. (A) Whole-cell patch-clamp was used to measure ionic current generated by Kv1.2 channels expressed in HEK293 cells. Top, a family of current traces evoked by voltage pulses from −70 to +40 mV in 10-mV increments in cells treated with either saline or with 10 μM carbachol. The traces are the average of 14 individual cells and show a significant suppression of Kv1.2 current ($p < 0.001$). Bottom, an identical experiment in cells expressing a mutant form of Kv1.2 (Y132F) shown previously in to resist tyrosine phosphorylation. These channels exhibit no significant carbachol-induced current suppression. (B) A parallel set of flow cytometry experiments measuring surface Kv1.2 levels reveal loss of Kv1.2 from the surface of cells expressing Kv1.2-WT but not from those expressing Kv1.2-Y132F. This indicates that the Y132F mutant channels are resistant to stimulus-induced channel endocytosis. Bars depict mean values from nine experiments ± SEM and normalized to saline control. (C-F) Cells expressing Y132F channels were analyzed by immunofluoresence to detect colocalization with the early endosomal marker EEA1. Entry of Kv1.2-Y132F channels into EEA1-labeled compartments was not observed in cells treated with saline (C), pervanadate (D) or carbachol (E) as described above. Insets, individual channels labeling Kv1.2-Y132F (green), EEA1 (red), or cortical actin (blue). (F) Quantitative analysis of the immunofluoresence data reveals that the number of cells scored as showing surface Kv1.2-Y132F labeling (black bar) is greater than those showing internalized (punctuate) colabeling of Kv1.2-Y132F with EEA1 (gray bar). (G) Stimulus-induced loss of surface Kv1.2 was detected biochemically by immunoprecipitation of surface Kv1.2 with anti-Kv1.2e polyclonal antibody. Immunoprecipitations were performed with control and pervanadate-treated HEK293 cells transiently expressing Kv1.2wt or Kv1.2-Y132F. Left, representative Western blots of immunoprecipitated surface Kv1.2 (IP) and total cell lysate (Lysate) probed with anti-Kv1.2 mAb; right, summarized data in which band densities were quantified and normalized to control. Each bar represents the mean of at least seven individual experiments ± SEM. Pervanadate potently reduced surface levels of transiently transfected Kv1.2wt to a degree similar to that observed in the stable cell line. In contrast, pervanadate had little effect on Kv1.2-Y132F surface expression.

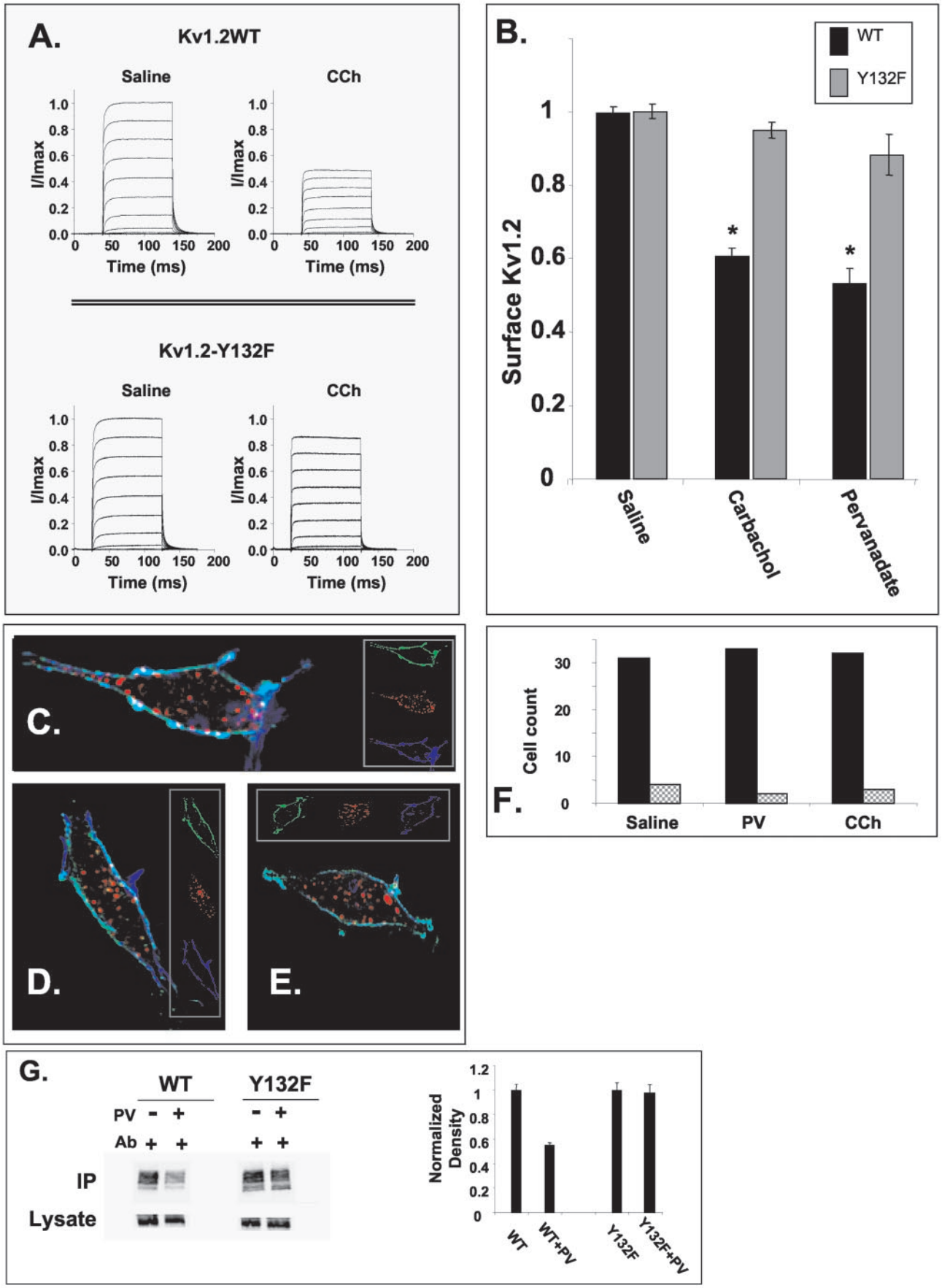
A.
Kv1.2WT
Saline
CCh
I/Imax
Time (ms)
Kv1.2-Y132F
B.
WT
Y132F
Surface Kv1.2
Saline
Carbachol
Pervanadate
C.
D.
E.
F.
Cell count
Saline
PV
CCh
G.
WT
Y132F
PV
Ab
IP
Lysate
Normalized Density
WT
WT+PV
Y132F
Y132F+PV

Figure 7.

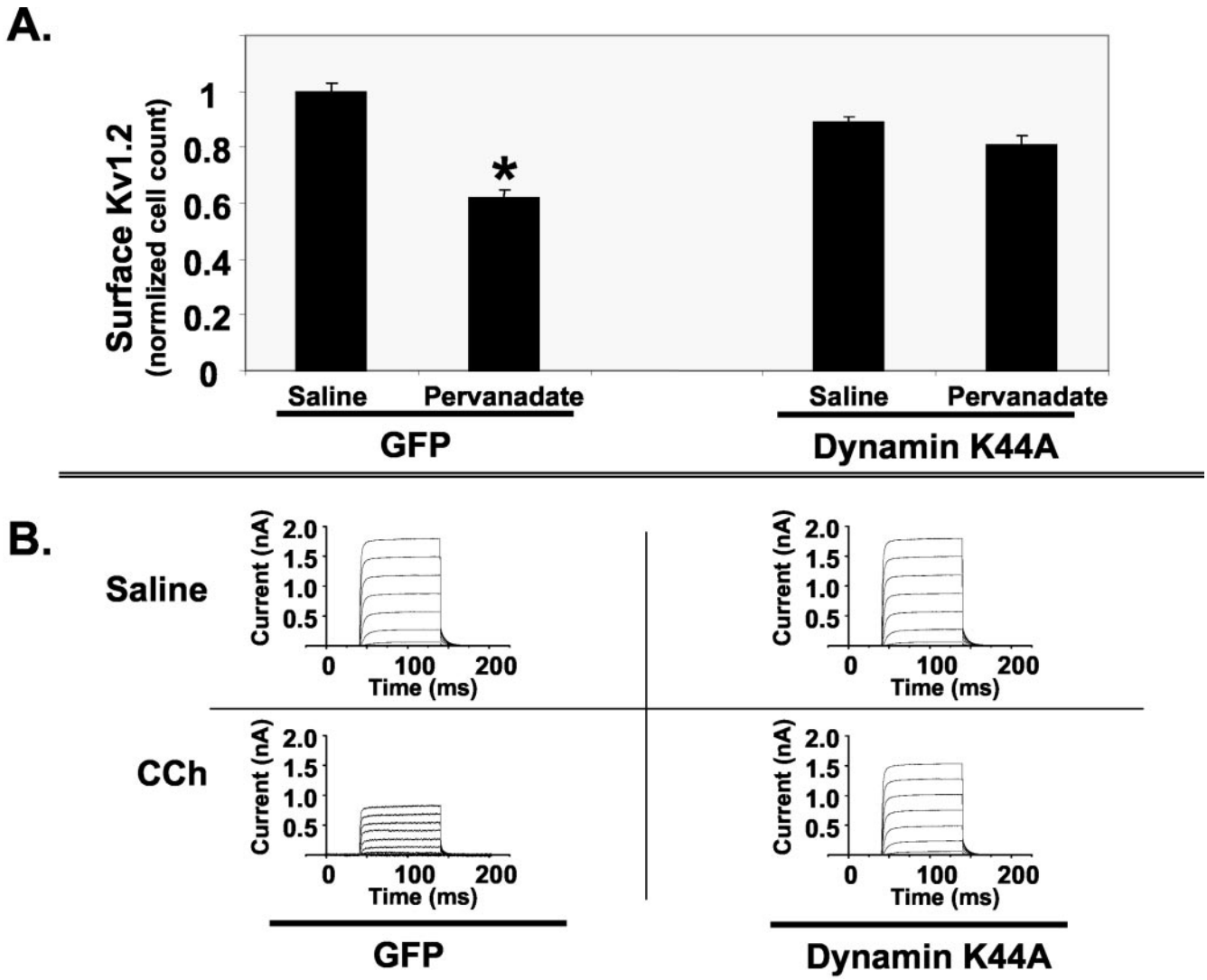

Figure 8. Dynamin is necessary for both Kv1.2 endocytosis and for suppression of Kv1.2 ionic current. (A) Detection of surface Kv1.2 by flow cytometry in GFP transfected cells treated with saline or pervanadate reveals that GFP alone does not interfere with pervanadate (32 μM, 10 min) induced loss of surface channel. Bars represent mean ± SEM normalized to saline control values (n = 9). Asterisk indicates significant reduction in Kv1.2 surface expression ($p < 0.0001$). In contrast, transfection of GFP + Dynamin K44A blocked pervanadate-induced surface channel loss ($p > 0.2$). (B) A parallel set of experiments measuring ionic current amplitude in cells transfected with GFP or with GFP + Dynamin K44A reveals that carbachol induces a significant suppression of Kv1.2 ionic current in cells expressing GFP alone relative to saline (n = 8, $p < 0.003$). In contrast, no significant difference is observed between the mean current amplitudes of saline vs. CCh-treated cells expressing the dominant negative form of dynamin (n = 15, $p > 0.1$).

Dynamin Mediates Both Channel Endocytosis and Suppression

Endocytosis occurs through a variety of different mechanisms, some dependent on clathrin (Takei and Haucke, 2001), others dependent on caveolin (Pelkmans and Helenius, 2002), and still others dependent on neither (Nichols and Lippincott-Schwartz, 2001). In many but not all cases, the GTP-binding protein dynamin appears to have a key role in the early stages of endocytosis and overexpression of GTPase deficient forms of dynamin (dynK44A) can inhibit endocytosis (Herskovits *et al.*, 1993). This form of dominant negative dynamin therefore provides a powerful tool with which to explore both the mechanism of Kv1.2 endocytosis and to further establish the causal relationship between Kv1.2 endocytosis and stimulus mediated suppression of Kv1.2 ionic current. We therefore assessed the effect of over-expressed dynK44A on stimulus-induced Kv1.2 endocytosis and current suppression.

To accomplish this, we transiently expressed either GFP alone or GFP + dynK44A in the HEK293 cell line expressing Kv1.2 and M1 receptors. Figure 8A shows that treatment with 32 μM pervanadate for 10 min caused a significant reduction in surface Kv1.2 levels in cells expressing GFP alone. However, identical treatment with pervanadate of cells expressing dynK44A had no significant effect on Kv1.2 surface expression. Therefore, the stimulus-induced endocytosis of Kv1.2 appears to proceed through a mechanism that requires dynamin. A parallel set of experiments shown in Figure 8B shows that expression of GFP alone had no effect on carbachol (10 μM) induced suppression of Kv1.2 ionic current, but that cells coexpressing GFP and dynK44A were resistant to such suppression. Therefore, endocytosis of

Kv1.2 proceeds in a dynamin-dependent manner and blocking such endocytosis also blocks stimulus mediated suppression of Kv1.2 ionic current. This strongly suggests a direct relationship between channel endocytosis and channel suppression.

DISCUSSION

Ion channels are the primary determinants of membrane excitability in most cells and are regulated to maintain membrane potential within specific parameters. Most often this occurs through modulation of the ion channel's function in response to extracellular stimuli. Direct phosphorylation of the channel protein by serine/threonine kinases is a well-studied means by which ion channels are regulated. Although in most cases the precise mechanisms for how serine/threonine phosphorylation affects channel function are not clear, the most commonly suggested mechanism is that phosphorylation-induced changes in channel structure alter the channel's structural or biophysical properties (Levitan, 1994). More recently, phosphorylation by tyrosine kinases has also been identified as an important means of ion channel regulation. The delayed rectifier potassium channel Kv1.2 was the first example of a voltage-gated ion channel so regulated (Huang *et al.,* 1993), and since then a range of voltage- and ligand-gated channels have been found to be regulated by tyrosine kinases, including NMDA receptors, voltage-gated calcium channels, and a variety of potassium channels (Spector *et al.,* 1983; Davis *et al.,* 2001). Importantly, Kv1 family channels in addition to Kv1.2 have been shown to undergo tyrosine kinase-dependent regulation as well, the most well studied of which are Kv1.3 and Kv1.5 (Holmes *et al.,* 1996a, 1996b; Fadool *et al.,* 1997; Fadool and Levitan, 1998). Discovery of this mode of channel regulation was particularly exciting because it revealed that the array of tyrosine kinase-dependent signaling systems primarily understood in terms of processes such as development, proliferation, motility and adhesion, could integrate with the array of signaling systems involved with the acute regulation of membrane potential. This has significant implications for processes ranging from development to neuronal plasticity.

Despite its importance, however, the mechanism by which tyrosine kinases modulate ion channels is limited. The picture is somewhat more clear for non-voltage-gated ion channels. The epithelial sodium channel EnaC is regulated, in part, through Nedd4-mediated ubiquitination in a process involving the interaction of a Nedd4 WW domain with a phosphotyrosine motif within the channel. The inward rectifying potassium channel Kir1.1 is also regulated by tyrosine kinases in a process involving dynamin- and clathrin-dependent channel endocytosis (Sterling *et al.,* 2002). Indeed, this finding provides an important perspective into the data reported here. Although Kv1.2 and Kir1.1 are both potassium channels that influence membrane excitability in a wide range of cells, they are structurally and phylogenetically distinct. The fact that such diverse potassium channels both appear to undergo tyrosine phosphorylation-dependent endocytosis suggest that this mechanism may be a widespread means of regulating membrane excitability.

The mechanism for regulating voltage-gated ion channels by tyrosine phosphorylation is less clear. Kv1.5 modulation by tyrosine kinases involve the SH3 domain-mediated physical interaction of src kinase with the channel protein (Holmes *et al.,* 1996b). Interestingly, the mechanism of this modulation appears to be multifaceted because the interaction itself, even in the absence of catalytic src activity, is sufficient to modulate channel function (Nitabach *et al.,* 2002). Further, Kv1.2 does not appear to interact with Src in this way, suggesting somewhat different mechanisms for Kv1.2 vs. Kv1.5 regulation. Kv1.3 is also regulated by tyrosine kinases, but a study examining the possible internalization of Kv1.3 as a mechanism of channel suppression yielded negative results (Fadool *et al.,* 1997). However, that interpretation may have been limited by the methodological scope of the experiments themselves. Changes in the level of surface Kv1.3 were inferred from differential antibody labeling of surface vs. internal Kv1.3 followed by detection with indirect immunofluoresence. Quantification of that data was limited to a relatively small sample size and may therefore have been unable to detect small but significant changes in surface channel levels.

In the studies presented here, changes in Kv1.2 surface expression were assayed using a variety of more sensitive techniques, including biochemical and flow cytometric studies capable of measuring surface Kv1.2 in thousands of cells per experiment. Using those methods, we find that tyrosine kinase-dependent modulation of Kv1.2 involves the regulated trafficking of the channel from the plasma membrane. This implies that tyrosine kinase-mediated endocytosis is a mechanism for effecting acute changes in membrane excitability associated with Kv1.2 suppression, including hyperexcitability associated with seizure in the cerebral cortex (Lambe and Aghajanian, 2001) as well as changes in smooth muscle excitability associated with hypertension (Kerr *et al.,* 2001; Thorneloe *et al.,* 2001; Lu *et al.,* 2002).

The initial indication that the levels of Kv1.2 within the plasma membrane might be regulated by posttranslational modification came from the observation that surface Kv1.2 levels varied independently of the total Kv1.2 expressed within unstimulated cells (Figure 1). Surface expression of Kv1.2 can also be enhanced by the Kvβ2 subunit, which influences Kv1.2 trafficking to the plasma membrane in some situations (Shi *et al.,* 1996; Trimmer, 1998). However, because the Kvβ2 subunit was stably expressed along with Kv1.2 in the cell line used in these studies, we surmised that another mechanism for differential Kv1.2 surface expression was at play, leading to the discovery that surface-expressed Kv1.2 undergoes stimulus-induced endocytosis. Thus, Kv1.2 surface expression is under two forms of regulatory control, one involving the Kvβ2-dependent trafficking of newly synthesized channel to the plasma membrane and the other involving stimulus-induced trafficking of the channel from the plasma membrane through endocytosis. Whether the two processes are related is unclear. We note that Kv1.2 endocytosis does occur in hippocampal neurons transfected with Kv1.2 alone (Figure 4), suggesting that stoichiometric levels of Kvβ2 may not be required for channel endocytosis in neurons. This parallels in vivo knockout studies suggesting that, in contrast to the case in heterologous expression systems (Shi *et al.,* 1996), Kvβ2 is not required for efficient maturation and trafficking of native Kv1.2 in neurons (McCormack *et al.,* 2002). McCormack *et al.* (2002) suggest several plausible explanations for that difference, including the compensatory expression of functionally similar beta subunit isotypes, developmental dependency of Kvβ2 effects, or a beta-subunit-independent mechanism for Kv1.2 trafficking to the plasma membrane in neurons. Regarding the latter possibility, McCormack *et al.* note that, in contrast to the exclusive expression of the Kv1.2-alpha subunit in a heterologous system, native expression of Kv1.2 is often accompanied by expression of other Kv1 alpha subunits, some of which may replace Kvβ2 in effecting Kv1.2 trafficking to the cell surface (Manganas and Trimmer, 2000). Therefore, Kvβ2 may be required to observe endocytosis in heterologous

expression systems only insofar is it is required for efficient maturation and surface expression of Kv1.2 in such systems. Nevertheless, we have not yet examined in depth the role of Kvβ2 in Kv1.2 regulation and its potential role in some aspects of Kv1.2 endocytosis remains an open question.

Our next goal was to determine whether endocytosis of Kv1.2 was directly related to suppression of Kv1.2 ionic current. Conversion of the N-terminal tyrosine 132 to phenylalanine partially inhibits receptor-mediated Kv1.2 tyrosine phosphorylation and ionic current suppression (Huang *et al.,* 1993). The finding that Kv1.2 channels harboring the Y132F mutation also resist endocytosis (Figure 6) supports the parsimonious hypothesis that channel suppression is caused by endocytosis. Introducing the Y132F mutation within Kv1.2 is unlikely to affect all endocytosis within the cell; thus, the stimulus-induced endocytosis of Kv1.2 is specific to the tyrosine-phosphorylated channel. It is important to note that Y132 is not the only tyrosine likely to contribute to Kv1.2 suppression by tyrosine phosphorylation. For example, the C-terminal tyrosines Y415 and Y417 have a key role in cortactin binding to Kv1.2 and strongly influence Kv1.2 ionic current levels (Hattan *et al.,* 2002). Their role in endocytosis awaits further study; however, the fact that they have a role in Kv1.2 physiology points toward a mechanism for channel endocytosis that is more complex than one involving the phosphorylation of a single tyrosine. It is intriguing to speculate that phosphorylation of a given tyrosine within Kv1.2 may trigger entry of the channel into the endocytotic pathway, whereas phosphorylation of other tyrosines may determine its trafficking fate within that pathway.

The finding that Y132F channels are resistant to both channel suppression and endocytosis supports a model in which Kv1.2 suppression is the result of channel endocytosis. However, that finding is also consistent with a less direct model in which endocytosis may affect a population of Kv1.2 channels on the cell surface that are distinct from those actively contributing to ionic current in the cell. In such a model, tyrosine phosphorylation would have two effects, first to suppress Kv1.2 ionic current, potentially by affecting the conformation of the protein, and second to signal the removal of suppressed channels from the plasma membrane through endocytosis. If this model were correct, we would hypothesize that specific inhibition of the endocytotic machinery would reduce receptor-mediated loss of surface Kv1.2 without blocking receptor-mediated channel suppression. However, our finding that inhibition of endocytosis with dynaminK44A blocked both channel endocytosis and suppression (Figure 8) argues against this idea. We therefore conclude that, although other mechanisms may be involved, receptor-mediated endocytosis is a significant component of the overall mechanism for the tyrosine phosphorylation-dependent suppression of Kv1.2 ionic current.

We also note that of all of the related Kv1 family channels, only Kv1.2 has a tyrosine at the cognate Y132 site. All others have a phenylalanine at the cognate position. Nevertheless, other Kv1 family channels undergo tyrosines phosphorylation-dependent suppression. A straightforward explanation is that the mechanism of suppression may be fundamentally different between the Kv1 family members. This possibility is especially important to consider in view of the findings of Fadool *et al.* (1997), in which the suppression Kv1.3 appears not to involve channel internalization. However, Kv1 family channels also share a number of common tyrosines, in particular Y415 and Y417, which may also have key roles in channel suppression (Hattan *et al.*, 2002). Thus, an alternative interpretation is that Y132 may have a regulatory role specific to Kv1.2 that is not present in other Kv1 family members. For example, phosphorylation of tyrosines other than Y132 may be the immediate trigger for endocytosis in Kv1 family channels. In Kv1.2, the phosphorylation of those tyrosines may be regulated by the phosphorylation state of Y132, whereas such regulation is absent in other Kv1 family channels. In this model, other Kv1 family channels could undergo tyrosine phosphorylation-dependent suppression by the same general mechanism as Kv1.2 but without the added level of control present in Kv1.2. Nevertheless, the data presented here indicates that Y132 has an important if not exclusive role in the suppression and endocytosis of Kv1.2.

What is the molecular mechanism of Kv1.2 endocytosis? In a previous study we found that Kv1.2 interacts directly with the actin binding protein cortactin and that the interaction is disrupted by channel tyrosine phosphorylation (Hattan *et al.,* 2002). In that same study we presented evidence that disruption of the Kv1.2-cortactin interaction may have a role in channel suppression. If so, regulated cortactin binding to Kv1.2 might also have a role in Kv1.2 endocytosis. One indication that this may be the case comes from the finding that disruption of the actin cytoskeleton with latrunculin is itself sufficient to cause channel endocytosis (Figure 6). For proteins in which surface expression is highly dependent on a stable interaction with the actin cytoskeleton, F-actin disruption might be expected to facilitate internalization. Because latrunculin caused internalization of Kv1.2, we posit that surface expressed Kv1.2 is tethered to F-actin and that such tethering key to maintaining the channel at the cell surface. Disrupting that interaction would free the channel to undergo endocytosis and consequent suppression. This interpretation is consistent with our finding that dissociation of cortactin from Kv1.2 is correlated with channel suppression, but that gross disruption of F-actin is not required for channel endocytosis (Figure 5). Thus, whether by channel phosphorylation-induced cortactin dissociation or by disruption of F-actin, dissociation of Kv1.2 from the actin cytoarchitecture appears to be a component of channel suppression.

Beyond its role in binding to F-actin, cortactin is a particularly interesting potential participant in Kv1.2 endocytosis because of its multiple other functions. Cortactin interacts directly with dynamin (Wu and Parsons, 1993) and is thought to contribute to endocytosis through that interaction and has also been found to localize to clathrin-coated pits and to contribute to clathrin-dependent endocytosis (Cao *et al.,* 2003). Thus, the fact that dynamin is a key component in the process of Kv1.2 regulation is perhaps not surprising in view of our previous finding that it is also a Kv1.2 binding partner. Equally interesting is the fact that cortactin harbors docking sites for SH2 domains within src and related kinases (Okamura and Resh, 1995). Thus cortactin may coordinate the interaction of Kv1.2 with the actin cytoskeleton to stabilize its expression on the cell surface but may also coordinate its interaction with other proteins required for its tyrosine kinase-dependent endocytosis.

ACKNOWLEDGMENTS

Flow cytometry was performed in the Vermont Cancer Center Flow Cytometry Facility and was supported in part by Grant P30CA22435 from the National Cancer Institute. We thank Scott Tighe for his assistance with those experiments. We also thank Dr. Lis Barfod for helpful discussions. This work was supported by National Institutes of Health Grant 1P20RR16435 (to A.D.M).

REFERENCES

Alkon, D.L., Nelson, T.J., Zhao, W., and Cavallaro, S. (1998). Time domains of neuronal Ca2+ signaling and associative memory: steps through a calexcitin, ryanodine receptor, K+ channel cascade. Trends Neurosci. *21*, 529–537.

Burke, N.A., Takimoto, K., Li, D., Han, W., Watkins, S.C., and Levitan, E.S. (1999). Distinct structural requirements for clustering and immobilization of K+ channels by PSD-95. J. Gen. Physiol. *113*, 71–80.

Cachero, T.G., Morielli, A.D., and Peralta, E.G. (1998). The small GTP-binding protein RhoA regulates a delayed rectifier potassium channel. Cell *93*, 1077–1085.

Cao, H., Orth, J.D., Chen, J., Weller, S.G., Heuser, J.E., and McNiven, M.A. (2003). Cortactin is a component of clathrin-coated pits and participates in receptor-mediated endocytosis. Mol. Cell. Biol. *23*, 2162–2170.

Carroll, R.C., Beattie, E.C., von Zastrow, M., and Malenka, R.C. (2001). Role of AMPA receptor endocytosis in synaptic plasticity. Nat. Rev. Neurosci. *2*, 315–324.

Carroll, R.C., Beattie, E.C., Xia, H., Luscher, C., Altschuler, Y., Nicoll, R.A., Malenka, R.C., and von Zastrow, M. (1999). Dynamin-dependent endocytosis of ionotropic glutamate receptors. Proc. Natl. Acad. Sci. USA *96*, 14112–14117.

Cayabyab, F.S., Khanna, R., Jones, O.T., and Schlichter, L.C. (2000). Suppression of the rat microglia Kv1.3 current by src-family tyrosine kinases and oxygen/glucose deprivation. Eur. J. Neurosci. *12*, 1949–1960.

Colley, B., Tucker, K., and Fadool, D.A. (2004). Comparison of modulation of Kv1.3 channel by two receptor tyrosine kinases in olfactory bulb neurons of rodents. Receptors Channels *10*, 25–36.

Davis, M.J., Wu, X., Nurkiewicz, T.R., Kawasaki, J., Gui, P., Hill, M.A., and Wilson, E. (2001). Regulation of ion channels by protein tyrosine phosphorylation 6. Am. J. Physiol. Heart Circ. Physiol. *281*, H1835–H1862.

Delaney, K.A., Murph, M.M., Brown, L.M., and Radhakrishna, H. (2002). Transfer of M2 muscarinic acetylcholine receptors to clathrin-derived early endosomes following clathrin-independent endocytosis. J. Biol. Chem. *277*, 33439–33446.

Derst, C., Konrad, M., Kockerling, A., Karolyi, L., Deschenes, G., Daut, J., Karschin, A., and Seyberth, H.W. (1997). Mutations in the ROMK gene in antenatal Bartter syndrome are associated with impaired K+ channel function. Biochem. Biophys. Res. Commun. *230*, 641–645.

Edwardson, J.M., and Szekeres, P.G. (1999). Endocytosis and recycling of muscarinic receptors. Life Sci. *64*, 487–494.

Fadool, D.A., Holmes, T.C., Berman, K., Dagan, D., and Levitan, I.B. (1997). Tyrosine phosphorylation modulates current amplitude and kinetics of a neuronal voltage-gated potassium channel. J. Neurophysiol. *78*, 1563–1573.

Fadool, D.A., and Levitan, I.B. (1998). Modulation of olfactory bulb neuron potassium current by tyrosine phosphorylation. J. Neurosci. *18*, 6126–6137.

Fadool, D.A., Tucker, K., Phillips, J.J., and Simmen, J.A. (2000). Brain insulin receptor causes activity-dependent current suppression in the olfactory bulb through multiple phosphorylation of Kv1.3. J. Neurophysiol. *83*, 2332–2348.

Hattan, D., Nesti, E., Cachero, T.G., and Morielli, A.D. (2002). Tyrosine phosphorylation of Kv1.2 modulates its interaction with the actin-binding protein cortactin. J. Biol. Chem. *277*, 38596–38606.

Herskovits, J.S., Burgess, C.C., Obar, R.A., and Vallee, R.B. (1993). Effects of mutant rat dynamin on endocytosis. J. Cell Biol. *122*, 565–578.

Higuchi, H., Takeyasu, K., Uchida, S., and Yoshida, H. (1982). Mechanism of agonist-induced degradation of muscarinic cholinergic receptor in cultured vas deferens of guinea-pig. Eur. J. Pharmacol. *79*, 67–77.

Holmes, T.C., Fadool, D.A., and Levitan, I.B. (1996a). Tyrosine phosphorylation of the Kv1.3 potassium channel. J. Neurosci. *16*, 1581–1590.

Holmes, T.C., Fadool, D.A., Ren, R., and Levitan, I.B. (1996b). Association of Src Tyrosine kinase with a human potassium channel mediated by SH3 domain. Science *274*, 2089–2094.

Huang, X.Y., Morielli, A.D., and Peralta, E.G. (1993). Tyrosine kinase-dependent suppression of a potassium channel by the G protein-coupled m1 muscarinic acetylcholine receptor. Cell *75*, 1145–1156.

Ince, C., Coremans, J.M., Ypey, D.L., Leijh, P.C., Verveen, A.A., and van Furth, R. (1988). Phagocytosis by human macrophages is accompanied by changes in ionic channel currents. J. Cell Biol. *106*, 1873–1878.

Ismailov, I.I., and Benos, D.J. (1995). Effects of phosphorylation on ion channel function. Kidney Int. *48*, 1167–1179.

Jeng, R.L., and Welch, M.D. (2001). Cytoskeleton: actin and endocytosis–no longer the weakest link. Curr. Biol. *11*, R691–R694.

Kerr, P.M., Clement-Chomienne, O., Thorneloe, K.S., Chen, T.T., Ishii, K., Sontag, D.P., Walsh, M.P., Cole, W.C. (2001). Heteromultimeric Kv1.2-Kv1.5 channels underlie 4-aminopyridine-sensitive delayed rectifier K(+) current of rabbit vascular myocytes. Circ. Res. *89*, 1038–1044.

Lambe, E.K., and Aghajanian, G.K. (2001). The role of Kv1.2-containing potassium channels in serotonin-induced glutamate release from thalamocortical terminals in rat frontal cortex. J. Neurosci. *21*, 9955–9963.

Lev, S., Moreno, H., Martinez, R., Canoll, P., Peles, E., Musacchio, J.M., Plowman, G.D., Rudy, B., Schlessinger, J. (1995). Protein tyrosine kinase P.Y.K2 involved in Ca(2+)-induced regulation of ion channel and M.A.P. kinase functions [see comments]. Nature *376*, 737–745.

Levitan, I.B. (1994). Modulation of ion channels by protein phosphorylation and dephosphorylation. Annu. Rev. Physiol. *56*, 193–212.

Lu, Y., Hanna, S.T., Tang, G., and Wang, R. (2002). Contributions of Kv1.2, Kv1.5 and Kv2.1 subunits to the native delayed rectifier K(+) current in rat mesenteric artery smooth muscle cells. Life Sci. *71*, 1465–1473.

Manganas, L.N., and Trimmer, J.S. (2000). Subunit composition determines Kv1 potassium channel surface expression. J. Biol. Chem. *275*, 29685–29693.

McCormack, K., Connor, J.X., Zhou, L., Ho, L.L., Ganetzky, B., Chiu, S.Y., and Messing, A. (2002). Genetic analysis of the mammalian K+ channel beta subunit Kvbeta 2 (Kcnab2). J. Biol. Chem. *277*, 13219–13228.

Moody, W.J. (1998). Control of spontaneous activity during development. J. Neurobiol. *37*, 97–109.

Mu, F.T. *et al*. (1995). EEA1, an early endosome-associated protein. EEA1 is a conserved alpha-helical peripheral membrane protein flanked by cysteine "fingers"and contains a calmodulin-binding IQ motif. J. Biol. Chem. *270*, 13503–13511.

Nichols, B.J., and Lippincott-Schwartz, J. (2001). Endocytosis without clathrin coats. Trends Cell Biol. *11*, 406–412.

Nitabach, M.N., Llamas, D.A., Araneda, R.C., Intile, J.L., Thompson, I.J., Zhou, Y.I., and Holmes, T.C. (2001). A mechanism for combinatorial regulation of electrical activity: Potassium channel subunits capable of functioning as Src homology 3-dependent adaptors. Proc. Natl. Acad. Sci. USA *98*, 705–710.

Nitabach, M.N., Llamas, D.A., Thompson, I.J., Collins, K.A., and Holmes, T.C. (2002). Phosphorylation-dependent and phosphorylation-independent modes of modulation of shaker family voltage-gated potassium channels by SRC family protein tyrosine kinases. J. Neurosci. *22*, 7913–7922.

Okamura, H., and Resh, M.D. (1995). p80/85 cortactin associates with the Src SH2 domain and colocalizes with v-Src in transformed cells 1. J. Biol. Chem. *270*, 26613–26618.

Olazabal, I.M., and Machesky, L.M. (2001). Abp1p and cortactin, new "handholds" for actin. J. Cell Biol. *154*, 679–682.

Pals-Rylaarsdam, R., Gurevich, V.V., Lee, K.B., Ptasienski, J.A., Benovic, J.L., and Hosey, M.M. (1997). Internalization of the m2 muscarinic acetylcholine receptor. Arrestin-independent and -dependent pathways. J. Biol. Chem. *272*, 23682–23689.

Pelkmans, L., and Helenius, A. (2002). Endocytosis via caveolae. Traffic *3*, 311–320.

Peralta, E.G., Ashkenazi, A., Winslow, J.W., Ramachandran, J., and Capon, D.J. (1988). Differential regulation of PI hydrolysis and adenyl cyclase by muscarinic receptor subtypes. Nature *334*, 434–437.

Qiu, M.H., Zhang, R., and Sun, F.Y. (2003). Enhancement of ischemia-induced tyrosine phosphorylation of Kv1.2 by vascular endothelial growth factor via activation of phosphatidylinositol 3-kinase. J. Neurochem. *87*, 1509–1517.

Qualmann, B., and Kessels, M.M. (2002). Endocytosis and the cytoskeleton. Int. Rev. Cytol. *220*, 93–144.

Rotin, D., Kanelis, V., and Schild, L. (2001). Trafficking and cell surface stability of ENaC. Am. J. Physiol. Renal Physiol. *281*, F391–F399.

Sah, V.P., Minamisawa, S., Tam, S.P., Wu, T.H., Dorn, G.W. 2, Ross, J.J., Chien, K.R., Brown, J.H. (1999). Cardiac-specific overexpression of RhoA. results in sinus and atrioventricular nodal dysfunction and contractile failure. J. Clin. Invest *103*, 1627–1634.

Schafer, D.A. (2002). Coupling actin dynamics and membrane dynamics during endocytosis. Curr. Opin. Cell Biol. *14*, 76–81.

Schild, L., Lu, Y., Gautschi, I., Schneeberger, E., Lifton, R.P., and Rossier, B.C. (1996). Identification of a PY motif in the epithelial Na channel subunits as a target sequence for mutations causing channel activation found in Liddle syndrome. EMBO J. *15*, 2381–2387.

Schlessinger, J., Shechter, Y., Willingham, M.C., and Pastan, I. (1978). Direct visualization of binding, aggregation, and internalization of insulin and epi-

dermal growth factor on living fibroblastic cells. Proc. Natl. Acad. Sci. USA *75*, 2659–2663.

Schliwa, M., Euteneur, U., Bulinski, J.C., and Izant, J.G. (1981). Calcium lability of cytoplasmic microtubules and its modulation by microtubule-associated proteins. Proc. Natl. Acad. Sci. USA *78*, 1037–1041.

Schmid, S.L., and Carter, L.L. (1990). ATP is required for receptor-mediated endocytosis in intact cells. J. Cell Biol. *111*, 2307–2318.

Sheng, M., and Kim, M.J. (2002). Postsynaptic signaling and plasticity mechanisms. Science *298*, 776–780.

Shi, G., Nakahira, K., Hammond, S., Rhodes, K.J., Schechter, L.E., and Trimmer, J.S. (1996). Beta subunits promote K+ channel surface expression through effects early in biosynthesis. Neuron *16*, 843–852.

Siegelbaum, S.A. (1994). Channel regulation. Ion channel control by tyrosine phosphorylation. Curr. Biol. *4*, 242–245.

Spector, I., Shochet, N.R., Blasberger, D., and Kashman, Y. (1989). Latrunculins–novel marine macrolides that disrupt microfilament organization and affect cell growth: I. Comparison with cytochalasin D. Cell Motil. Cytoskel. *13*, 127–144.

Spector, I., Shochet, N.R., Kashman, Y., and Groweiss, A. (1983). Latrunculins: novel marine toxins that disrupt microfilament organization in cultured cells. Science *219*, 493–495.

St John, P.A., and Gordon, H. (2001). Agonists cause endocytosis of nicotinic acetylcholine receptors on cultured myotubes. J. Neurobiol. *49*, 212–223.

Staub, O., Abriel, H., Plant, P., Ishikawa, T., Kanelis, V., Saleki, R., Horisberger, J.D., Schild, L., and Rotin, D. (2000). Regulation of the epithelial Na+ channel by Nedd4 and ubiquitination. Kidney Int. *57*, 809–815.

Staub, O., Gautschi, I., Ishikawa, T., Breitschopf, K., Ciechanover, A., Schild, L., and Rotin, D. (1997). Regulation of stability and function of the epithelial Na+ channel (ENaC) by ubiquitination. EMBO J. *16*, 6325–6336.

Sterling, H., Lin, D.H., Gu, R.M., Dong, K., Hebert, S.C., and Wang, W.H. (2002). Inhibition of protein-tyrosine phosphatase stimulates the dynamin-dependent endocytosis of ROMK1. J. Biol. Chem. *277*, 4317–4323.

Stevens, C.F., and Sullivan, J. (1998). Synaptic plasticity. Curr. Biol. *26*, 151–153.

Takei, K., and Haucke, V. (2001). Clathrin-mediated endocytosis: membrane factors pull the trigger. Trends Cell Biol. *11*, 385–391.

Thorneloe, K.S., Chen, T.T., Kerr, P.M., Grier, E.F., Horowitz, B., Cole, W.C., and Walsh, M.P. (2001). Molecular composition of 4-aminopyridine-sensitive voltage-gated K(+) channels of vascular smooth muscle. Circ. Res. *89*, 1030–1037.

Trimmer, J.S. (1998). Regulation of ion channel expression by cytoplasmic subunits. Curr. Opin. Neurobiol. *8*, 370–374.

Tsai, W., Morielli, A.D., Cachero, T.G., and Peralta, E.G. (1999). Receptor protein tyrosine phosphatase alpha participates in the m1 muscarinic acetylcholine receptor-dependent regulation of Kv1.2 channel activity. EMBO J. *18*, 109–118.

Tsai, W., Morielli, A.D., and Peralta, E.G. (1997). The m1 muscarinic acetylcholine receptor transactivates the EGF receptor to modulate ion channel activity. EMBO J. *16*, 4597–4605.

Vollmer, M., Koehrer, M., Topaloglu, R., Strahm, B., Omran, H., and Hildebrandt, F. (1998). Two novel mutations of the gene for Kir 1.1 (ROMK) in neonatal Bartter syndrome. Pediatr. Nephrol. *12*, 69–71.

Wilde, A., Beattie, E.C., Lem, L., Riethof, D.A., Liu, S.H., Mobley, W.C., Soriano, P., and Brodsky, F.M. (1999). EGF receptor signaling stimulates SRC kinase phosphorylation of clathrin, influencing clathrin redistribution and EGF uptake. Cell *96*, 677–687.

Wu, H., and Parsons, J.T. (1993). Cortactin, an 80/85-kilodalton pp60src substrate, is a filamentous actin-binding protein enriched in the cell cortex. J. Cell Biol. *120*, 1417–1426.

Zeng, W.Z., Babich, V., Ortega, B., Quigley, R., White, S.J., Welling, P.A., and Huang, C.L. (2002). Evidence for endocytosis of ROMK potassium channel via clathrin-coated vesicles. Am. J. Physiol. Renal Physiol. *283*, F630–F639.

Zhou, J., Valletta, J.S., Grimes, M.L., and Mobley, W.C. (1995). Multiple levels for regulation of TrkA in PC12 cells by nerve growth factor. J. Neurochem. *65*, 1146–1156.